

Heart Development and Congenital Structural Heart Defects

Lucile Houyel^{1,2} and Sigolène M. Meilhac^{2,3}

¹Unité de Cardiologie Pédiatrique et Congénitale and Centre de Référence des Malformations Cardiaques Congénitales Complexes (M3C), Hôpital Necker-Enfants Malades, Assistance Publique-Hôpitaux de Paris (AP-HP), 75015 Paris, France

²Université de Paris, 75015 Paris, France

³*Imagine*-Institut Pasteur Unit of Heart Morphogenesis, INSERM UMR 1163, 75015 Paris, France; email: sigolene.meilhac@institutimagine.org

Annu. Rev. Genom. Hum. Genet. 2021. 22:257–84

First published as a Review in Advance on
June 1, 2021

The *Annual Review of Genomics and Human Genetics*
is online at genom.annualreviews.org

<https://doi.org/10.1146/annurev-genom-083118-015012>

Copyright © 2021 by Annual Reviews. This work is licensed under a Creative Commons Attribution 4.0 International License, which permits unrestricted use, distribution, and reproduction in any medium, provided the original author and source are credited. See credit lines of images or other third-party material in this article for license information

ANNUAL
REVIEWS **CONNECT**

www.annualreviews.org

- Download figures
- Navigate cited references
- Keyword search
- Explore related articles
- Share via email or social media

Keywords

congenital heart defects, International Paediatric and Congenital Cardiac Code, ICD-11, heart morphogenesis, mouse models, embryonic heart, septal defects, conotruncal defects, laterality defects, valve defects

Abstract

Congenital heart disease is the most frequent birth defect and the leading cause of death for the fetus and in the first year of life. The wide phenotypic diversity of congenital heart defects requires expert diagnosis and sophisticated repair surgery. Although these defects have been described since the seventeenth century, it was only in 2005 that a consensus international nomenclature was adopted, followed by an international classification in 2017 to help provide better management of patients. Advances in genetic engineering, imaging, and omics analyses have uncovered mechanisms of heart formation and malformation in animal models, but approximately 80% of congenital heart defects have an unknown genetic origin. Here, we summarize current knowledge of congenital structural heart defects, intertwining clinical and fundamental research perspectives, with the aim to foster interdisciplinary collaborations at the cutting edge of each field. We also discuss remaining challenges in better understanding congenital heart defects and providing benefits to patients.

1. INTRODUCTION

Malformation of the heart is the most frequent congenital defect, affecting 1% of live births, and is a major cause of pregnancy termination and fetal death (61, 112). Congenital heart defects (CHDs) are a major public health issue: These defects are the leading cause of death in the first year of life, cause morbidity and hospitalization in children, and often require lifelong follow-up. Collectively, CHDs are common, but individually they may correspond to rare or ultrarare disorders, requiring expert diagnosis and sophisticated repair surgery.

The genetic origins of CHDs provide diagnostic tools and help families understand why their children are affected, but they remain unknown in approximately 80% of cases. These origins have been identified in syndromic forms (e.g., Down syndrome, 22q11.2 deletion, Holt–Oram syndrome, and Alagille syndrome) and in most cardiomyopathies (hypertrophic, dilated, and restrictive cardiomyopathies; left ventricular noncompaction; and arrhythmogenic right ventricular dysplasia) (112, 147). Beyond the molecular aspect, deciphering the embryological emergence of CHDs requires fundamental research to develop and analyze animal models. From the work of pioneering embryologists to contemporary research using the latest technological advances in genetic engineering, molecular screening, spatiotemporal imaging, and computational analyses, mechanisms of heart development relevant to CHDs have been uncovered in fish, chick, and mouse models. Knowledge of the pathophysiological mechanisms is crucial in order to target the cause of the disease beyond symptomatic management.

Addressing CHDs requires the integration of different types of expertise and, thus, interactions between clinicians (pediatric cardiologists, surgeons, anatomists, fetopathologists, radiologists, and obstetricians) and researchers (epidemiologists, geneticists, developmental biologists, and computational scientists). This review aims to promote such interactions by providing up-to-date knowledge of mammalian heart development mechanisms beyond the anatomical aspects that are usually covered by medical training. In addition, we summarize the rationale for the CHD nomenclature, since research articles that improperly phenotype CHDs prevent the utilization of mechanistic insights into diseases. We do not address cardiomyopathies or heart rhythm disorders (which impair the contractile function), the underlying mechanisms of myocardium growth and architecture, or the formation of the cardiac conduction system, innervation, and vascularization. We rather focus on structural CHDs (which impact the establishment of the double blood circulation) and the underlying mechanisms of cardiac compartmentalization.

2. NOMENCLATURE AND CLASSIFICATION OF CONGENITAL HEART DEFECTS

The majority of CHDs have been described and named since the seventeenth century. The first attempt to create a nomenclature was by Maude Abbott (1) in her *Atlas of Congenital Heart Disease*, in which she established the basis for all systems of classification of CHDs by describing the morphology of the most frequent individual lesions.

The study of postmortem cardiac specimens has led to enormous progress in the anatomical description of CHDs, mainly from the outstanding contributions of the pioneer cardiac anatomists Stella and Richard Van Praagh in Boston and Robert H. Anderson in London. In the segmental approach for the analysis of complex CHDs (137), as well as the sequential approach (4), the spatial positions of the main cardiac compartments (atria, ventricles, and great arteries) are described, as well as the connections and alignments between them. The fundamental principle of these approaches is that each segment should be analyzed independently, according to its morphology (**Table 1**). For example, the left ventricle is not defined based on its position on the left side or its functional contribution to the systemic circulation; rather, it is defined based on its own

Table 1 Segmental analysis of congenital heart defects

Segment	Letter	Description	Definition
Atria	S	Solitus	Morphological right atrium on the right, morphological left atrium on the left
	I	Inversus	Morphological right atrium on the left, morphological left atrium on the right
	A	Ambiguous	Impossibility of differentiating the two atria
Ventricles	D	D-loop	Morphological right ventricle on the right, morphological left ventricle on the left
	L	L-loop	Morphological right ventricle on the left, morphological left ventricle on the right
Great arteries (concordant ventriculo-arterial connections, usually spiraling great arteries)	S	Solitus	Aorta posterior and on the right, pulmonary artery anterior and on the left: 
	I	Inversus	Aorta posterior and on the left, pulmonary artery anterior and on the right: 
Great arteries (discordant ventriculo-arterial connections, usually parallel great arteries)	D	D-malposition	Aorta on the right of the pulmonary artery (usually anterior): 
	L	L-malposition	Aorta on the left of the pulmonary artery (usually anterior): 
	A	Anteroposterior malposition	Aorta strictly anterior to the pulmonary artery: 

Table based on information from Reference 137. In the great-arteries segments, the red circle represents the position of the aortic valve, and the black circle represents the position of the pulmonary valve, from a basal view of the heart.

morphology (smooth septal surface, fine apical trabeculations, and lack of septal attachments of the atrioventricular valve). To quote Anderson (3, p. 902), “when using the segmental approach to diagnosis. . . as modified to take note of the connections between the cardiac segments, even the most complex cardiac malformations can now be described in simple, accurate, and unambiguous fashion.” These approaches have thus been of great help to clinicians, enabling a huge step forward in the analysis of the various cardiac lesions. The segmental approach, commonly used in echocardiography by pediatric cardiologists, is also applicable to recent 3D imaging techniques, such as computed tomography (CT) scans or magnetic resonance imaging (MRI) performed by radiologists. Although the segmental analysis is invaluable for describing all the components of a given cardiac defect, it is not a classification and does not include the pooling of phenotypes into specific spectra, potentially reflecting a common pathophysiological mechanism.

CHDs exhibit considerable phenotypic diversity, and it is essential for clinicians to use the same terminology in the same way, so as to unify the diagnostic process and optimize the therapeutic management of patients (83). This need for standardization led to the creation, in 2005, of the International Paediatric and Congenital Cardiac Code (IPCCC), which can be viewed and downloaded at <http://www.ipccc.net>. Since then, the International Society for Nomenclature of Paediatric and Congenital Heart Disease (ISNPCHD) has developed, maintained, and updated the

IPCCC: International Paediatric and Congenital Cardiac Code

ISNPCHD: International Society for Nomenclature of Paediatric and Congenital Heart Disease

Table 2 The 10 major categories (level 1 terms) of congenital heart defects in the 11th iteration of the International Classification of Diseases

Number	Category
1	Congenital anomaly of position or spatial relationships of thoraco-abdominal organs (heterotaxy)
2	Congenital anomaly of an atrioventricular or ventriculo-arterial connection
3	Congenital anomaly of mediastinal veins (systemic and pulmonary veins)
4	Congenital anomaly of an atrium or atrial septum
5	Congenital anomaly of an atrioventricular valve or atrioventricular junction
6	Congenital anomaly of a ventricle or the ventricular septum
7	Functionally univentricular heart
8	Congenital anomaly of a ventriculo-arterial valve or adjacent regions
9	Congenital anomaly of great arteries including arterial duct
10	Congenital anomaly of coronary arteries

Table adapted from Reference 12.

thousands of entries of the IPCCC (12), reflecting a consensus view among anatomists, pediatric cardiologists, and surgeons. In 2010 and 2011, three classifications were published, taking into account physiology and anatomy (130), embryology and epidemiology (16), and anatomy and clinical management (54), the last of which incorporates IPCCC codes. More recently, the ISNPCHD, together with the World Health Organization, published a classification of CHDs that forms the CHD section of the 11th iteration of the International Classification of Diseases (ICD-11), which includes 318 terms with their definitions and synonyms (38); by comparison, the CHD section in previous versions of ICD was much less developed, including only 73 items in ICD-10 and 29 in ICD-9. The current 318 items are grouped into a tree view starting from 10 main categories (Table 2). The great advantage of ICD-11 is that it represents an international consensus about the classification and definitions of the most frequent CHDs in humans, providing a comprehensive and standardized system of coding and classification that is easy to use for clinicians, basic scientists, and administrators all over the world and has been translated into multiple languages (38).

Classification of CHDs aims to guide surgical and interventional treatment as well as medical management of patients and is key for epidemiological (61) and recurrence (36) studies. The grouping of phenotypes into large families of malformations is meant to provide insight into the underlying mechanisms and therefore reflect a specific developmental origin. Classification is thus not a definitive overview of CHDs and is likely to mature along with scientific discoveries. Recent classifications are not based on genetics, because a very small proportion of CHDs have an identified genetic cause, and most CHDs are sporadic. With advances in cardiac embryology, in the two last decades, mechanistic insights from animal models have been included in the most recent classifications. Most families of CHDs are due to a developmental anomaly in a specific cell population of the heart at a specific stage of cardiac development. This is best exemplified by the cardiac neural crest and anterior second heart field defects, commonly referred to as conotruncal defects. This group of CHDs includes common arterial trunk (CAT), tetralogy of Fallot with or without pulmonary atresia, outlet malalignment ventricular septal defects (VSDs), double-outlet right ventricle (DORV) with a subaortic or juxta-arterial VSD, and interrupted aortic arch (IAA) type B. Genetically, these defects can be associated with DiGeorge syndrome, caused by 22q11 microdeletions (including *Tbx1*), which is predominantly expressed and required in the anterior second heart field (151). During cardiac development, abnormal migration of cardiac neural crest cells compromises the addition of myocardial cells from the anterior second heart field. This impairs the elongation of the outflow tract and leads to various degrees of abnormal rotation and septation of the outflow tract, accounting for the spectrum of conotruncal defects (140)

ICD: International Classification of Diseases

CAT: common arterial trunk

DORV: double-outlet right ventricle

VSD: ventricular septal defect

IAA: interrupted aortic arch

(see Sections 3 and 4). Anatomically, all of these defects include an outlet VSD corresponding to various anomalies in the development and position of the outlet septum (102).

Some CHDs have been considered an arrest of development (136), in the sense that the pathological configuration is reminiscent of an earlier embryonic stage. DORV, for example, is the normal mode of ventriculo-arterial connection during heart development until the wedging stage, and double-inlet left ventricle is the normal mode of atrioventricular connection before the establishment of the right atrioventricular junction. By contrast, other defects have no developmental counterpart and thus seem to result from a deviating mechanism. This is the case for double-outlet left ventricle and double-inlet right ventricle.

It is important to note that families of CHDs comprise a continuum of defects with overlapping zones, introducing dynamics into the CHD nomenclature, which is reviewed occasionally. This has been well demonstrated for outflow tract malformations (**Figure 1**). In this group of CHDs, which have in common an outlet VSD, the rotation of the outflow tract is reflected anatomically by the position of the aorta relative to the left ventricle, and the spiraling of the great vessels. Variations in the rotation have been correlated with the different positions of the coronary arterial orifices on the aortic root, which vary according to the type of conotruncal defect, as well as with variation in the phenotype of the outlet VSD (53, 102). Such studies illustrate how a detailed anatomical analysis of the malformed human heart can corroborate embryological knowledge acquired from animal models. Another example is the classification of VSDs, as incorporated into ICD-11. This classification aimed to unify the terminology used to describe different categories of congenital cardiac malformations “in which there is a hole or pathway between the ventricular chambers,” according to the ISNPCHD definition (38, p. 1919). It is based primarily on the position of the hole relative to the anatomical landmarks on the right side of the ventricular septum, with four main categories (central perimembranous, inlet, trabecular muscular, and outlet VSDs; **Figure 2**), but also takes into account the borders of the defect, which are important indicators for the surgeon of the degree of vulnerability of the conduction pathways (83). This system of classification is consistent with the current knowledge of the development of the ventricular septum, with each of the four types of VSD corresponding to different developmental processes (7) (see Sections 3 and 4).

The mouse heart has a very similar anatomy to the human heart. Among the small differences is the venous return: Four pulmonary veins connect individually to the left atrium in humans, whereas they connect to an intermediate collector in the mouse. Unlike in humans, the left superior caval vein is persistent in mice and connects to the right atrium via a dilated coronary sinus. Atrial appendages have a distinct external shape only in humans—a triangular shape with a large orifice on the right, and a finger-like shape with a narrow orifice on the left. Differences between the trabeculation of the left and right interventricular septal surfaces are less obvious in mice. The septal band is difficult to detect on the septal surface of the mouse right ventricle, and the moderator band is higher and thinner than it is in the human heart. Apart from these variations, the clinical nomenclature of CHDs applies well to the mouse, making the mouse a good model to study the embryological mechanisms of CHDs. A thorough and accurate description of lesions in the many mouse models with CHDs is currently lacking in many research articles. Such descriptions are crucial to making relevant comparisons and thus to better deciphering the origins of CHDs.

3. HEART DEVELOPMENT

One function of the heart is to orchestrate a double blood circulation. This circulation relies on the partitioning of the heart into right and left halves, driving the pulmonary and systemic blood circulations, respectively. Failure to establish this partitioning impairs the oxygenation level of the

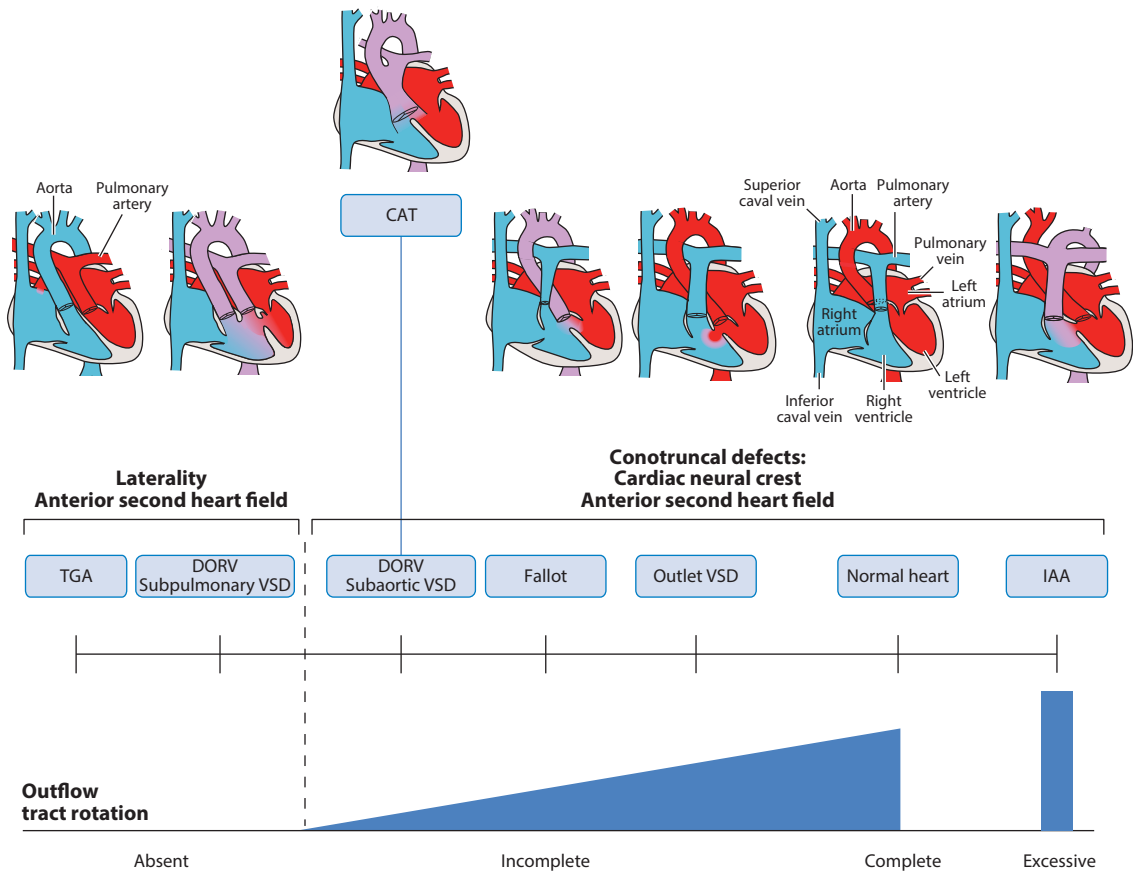


Figure 1

Spectrum of outflow tract defects, showing anomalies resulting from an abnormal rotation of the outflow tract, which may be absent (in DORV with a subpulmonary VSD, TGA, and CAT), incomplete (in DORV with a subaortic or doubly committed VSD, tetralogy of Fallot, or outlet malalignment VSD), or excessive (IAA type B). With the exception of some TGAs, these defects share the same anatomical type of VSD—namely, an outlet VSD with a malaligned and/or fibrous outlet septum. The anterior second heart field is involved in all outflow tract anomalies, in association with laterality abnormalities in TGA and DORV with a subpulmonary VSD, or in association with defective cardiac neural crest in a category commonly referred to as conotruncal defects. Abbreviations: CAT, common arterial trunk; DORV, double-outlet right ventricle; IAA, interrupted aortic arch; TGA, transposition of the great arteries; VSD, ventricular septal defect. We thank D. Rocancourt for the heart schemes.

blood, thus compromising organ functions. In the early embryo, the primordium of the heart is a tube, raising the question of how two circulations can emerge from a single tube.

3.1. Heart Patterning

Organogenesis is based on the coordination of cell behavior to shape tissues and position organs relative to each other. Thus, preceding the emergence of shape are molecular regulations that provide positional information to cells, a process referred to as patterning. This is usually based on gradients of morphogens, which activate transcriptional networks.

The heart tube forms at Carnegie stage 9 (CS9) in humans, at approximately 20 days of pregnancy (123), and embryonic day 8.5e (E8.5e) in mice, i.e., the ninth day of gestation (70) (Figure 3). Experiments in animal models have shown that the early heart tube is already

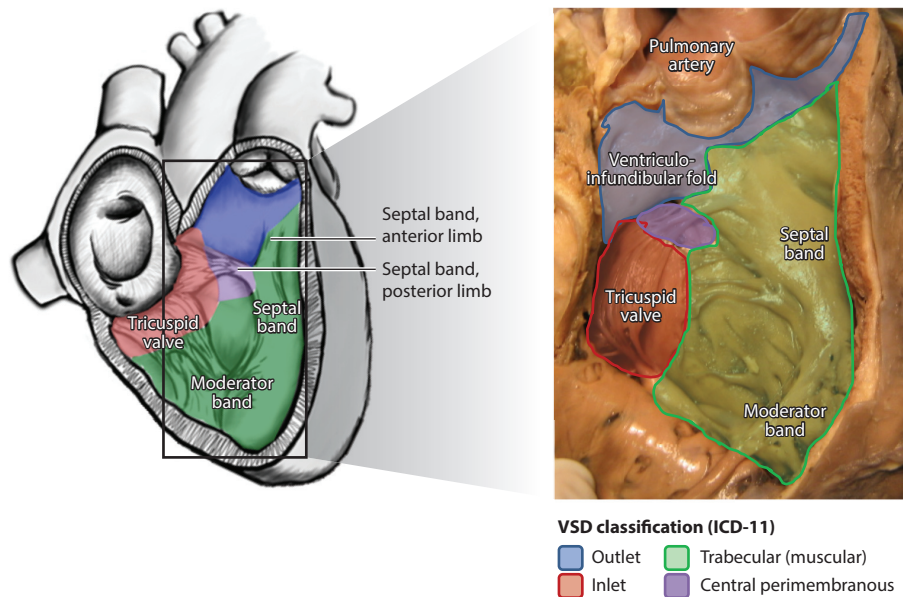


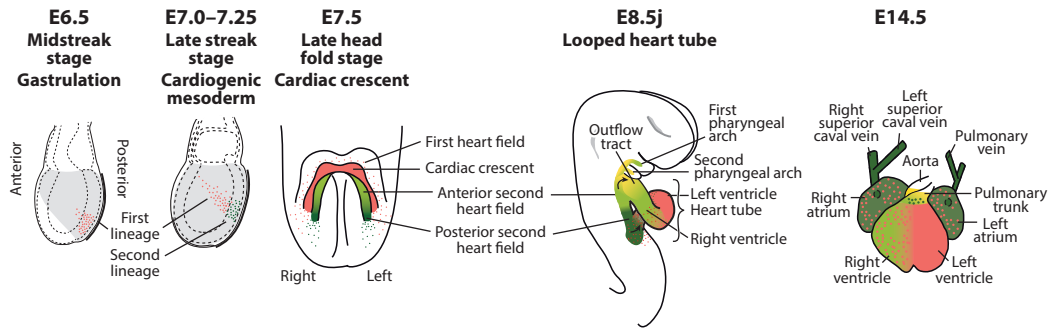
Figure 2

Classification of VSDs in ICD-11, showing a schematic representation and photograph of the septal surface in the human right ventricle. The outlet VSDs (*blue*) are cradled between the two limbs of the septal band and lie below the pulmonary valve. The inlet VSDs (*red*) are located behind the entire length of the septal leaflet of the tricuspid valve. The central perimembranous VSDs (*purple*) lie under the ventriculo-infundibular fold, behind the papillary muscle of the conus and behind the septal leaflet of the tricuspid valve. The trabecular VSDs (*green*) are located in the rest of the ventricular septum and can be anterior, posterior, midmuscular, basal, or apical. Abbreviations: ICD-11, 11th iteration of the International Classification of Diseases; VSD, ventricular septal defect. We thank G. André for the scheme.

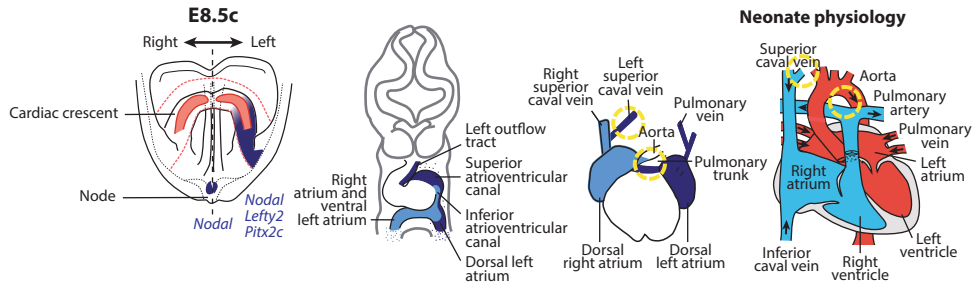
patterned, as are the neighboring cardiac precursor cells, which lie in the dorsal pericardial wall from an anatomical perspective, also referred to as the lateral plate mesoderm or heart field from an embryological perspective (**Figure 4**). Patterning of cardiac cells is not intuitive (i.e., does not follow the logic of functional or anatomical segmentation) but rather follows the embryonic signaling cascade and evolutionary constraints. Well before the heart tube forms, at the gastrulation stages (mouse E6.5 stage, equivalent to human CS7–8, at approximately 15–19 days of pregnancy), clonal analyses have revealed the existence of two populations of myocardial precursor cells, the first and second lineages (73, 91). These lineages, which ingress sequentially through the primitive streak, have overlapping contributions to the right ventricle, atrioventricular canal, and atria and a specific contribution to the left ventricle (first lineage) and outflow tract (second lineage). Recent advances in single-cell transcriptomics have refined the molecular definitions of these lineages (31), their dynamic localization at sequential stages in the first and second heart fields, and their routes and timing of incorporation into the heart tube (135).

Another patterning important for heart morphogenesis is left/right, initiated in the left/right organizer and mediated mainly by the secreted factor Nodal (105). Precisely timed gene expression analyses and drug treatments have shown that Nodal is required at E8.5c–d (i.e., before the formation of the heart tube) to specify a left identity in myocardial precursor cells (32). DiI labeling (34), clonal analyses (71, 72), and genetic tracing of *Nodal* (32) enable the contributions of the left/right second heart field to be traced: At E9.5, left precursors contribute to the left sinus venosus, the dorsal left atrium, the superior atrioventricular canal, and the left outflow tract, and at

a Myocardial lineages



b Left/right patterning



c Anteroposterior patterning

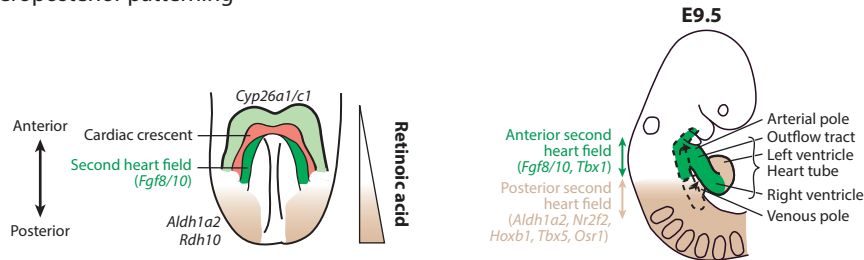


Figure 3

Mouse heart patterning. (a) First (red) and second (green) myocardial cell lineages ingress sequentially through the primitive streak at gastrulation. At E7.5, the first lineage has started differentiating into cardiomyocytes of the cardiac crescent, while the second lineage remains as progenitors in the second heart field. Further subdivisions (yellow, light green, and dark green) of the second heart field are shown at E8.5, along with their respective contributions to the fetal E14.5 heart. Colored dots indicate the regions of the heart with a dual origin. (b) Asymmetric Nodal signaling in the node and left lateral plate mesoderm is detected at E8.5c. Derivatives of the left (dark blue) and right (light blue) second heart fields are shown at E8.5j and E14.5. Discrepancies between the embryological left/right origin shown at E14.5 and the physiological left/right partitioning of the neonatal heart are outlined in yellow. (c) The anteroposterior gradient of retinoic acid signaling, produced by Aldh1a2- and Rdh10-synthesizing enzymes, is antagonized by the degrading enzymes Cyp26a1/c1 and Fgf signaling. This subdivides the second heart field at E9.5 into anterior and posterior domains, contributing to the arterial and venous poles, respectively. Lateral views are shown at E6.5, E7, E8.5 (in panel a), and E9.5, and frontal views are shown at E7.5, E8.5 (in panel b), and E14.5. Abbreviation: E, embryonic day.

E14.5, they contribute to the left superior caval vein, the pulmonary vein, the left atrium, and the pulmonary trunk. This indicates that the embryological left/right origin is not equivalent to the physiological left/right partitioning of blood circulation in the heart: The aorta belongs physiologically to the left segment of the heart (systemic circulation) but has a right origin, whereas the pulmonary trunk and left superior caval vein belong physiologically to the right heart (pulmonary circulation) but have a left origin. The left atrium has a double left/right origin (Figure 3b).

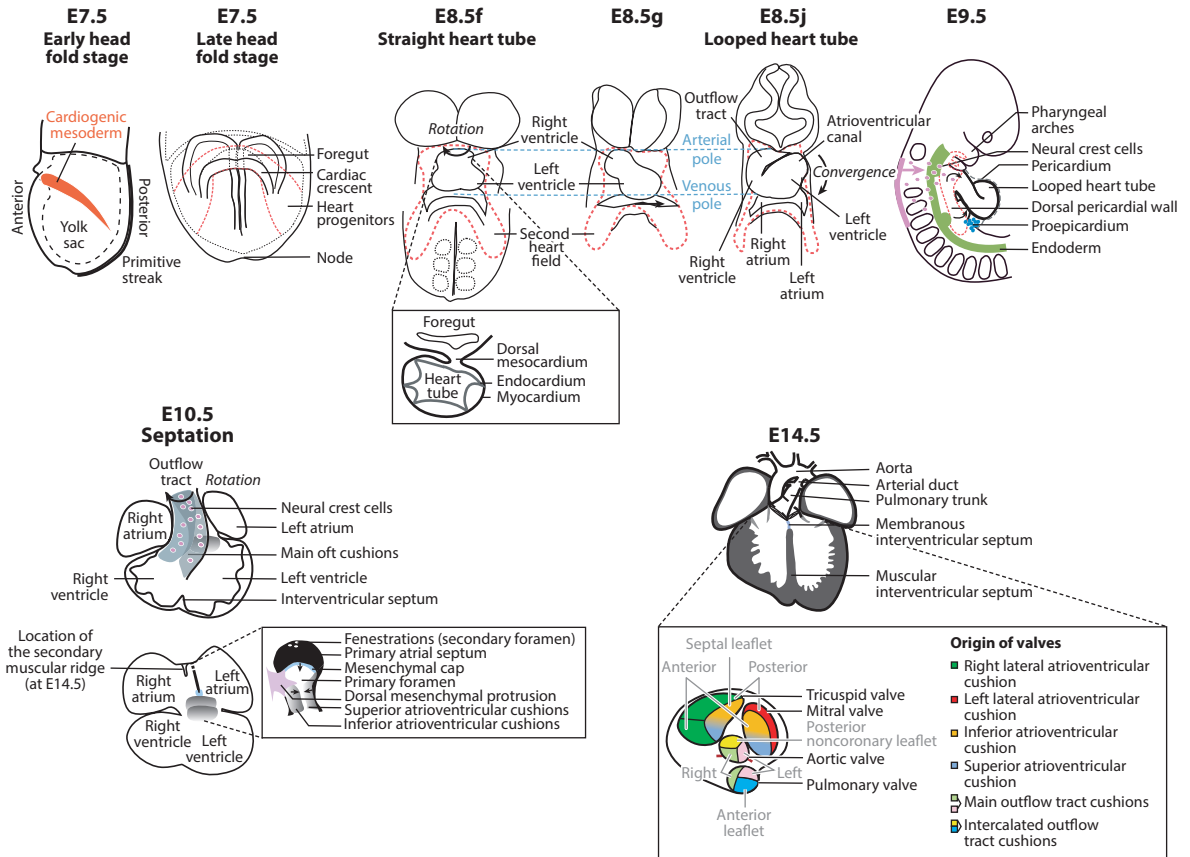


Figure 4

Mouse heart development. After gastrulation, cardiac progenitors migrate laterally toward the head folds at E7.5, where the cardiac crescent forms upon cardiomyocyte differentiation. At E8.5f, a straight heart tube composed of an inner layer of endocardium and an outer layer of myocardium (*inset*) elongates by incorporation of second heart field cells at both the arterial and venous poles. It is attached dorsally by the dorsal mesocardium (*inset*), which is progressively broken down as heart looping progresses. The arterial pole undergoes a rightward rotation (*arrow*), leading to the rightward tilting of the heart tube at E8.5g. Asymmetric cell ingressions result in the leftward displacement of the venous pole (*arrow*). At E8.5j, heart looping is complete, and the heart tube has acquired a helical shape. Later convergence of the heart tube poles is shown by an arrow. At E9.5, neural crest cells (*pink*) migrate toward the arterial pole, and the endoderm (*green*) is a source of Shh signaling. At E10.5, septation of the outflow tract, ventricles, and atria is underway. The outflow tract continues its rightward rotation. At E14.5, the aortic valve has wedged between the atrioventricular valves (*inset*). Septation is complete in the fetal heart, with the exception of bypasses at the level of the arterial duct and atrial secondary foramen. These bypasses are closed at birth, so that the double blood flow is established in the neonate heart. Lateral views are shown at E7.5 and E9.5, and frontal views are shown at other stages. Abbreviation: E, embryonic day.

Additional patterning along the anteroposterior axis regulates the spatiotemporal incorporation of cardiac precursor cells at the venous (posterior) and arterial (anterior) poles. An important determinant of this patterning is posterior retinoic acid signaling, which is antagonized by anterior Fgf signaling (14). Mouse mutant analyses and drug treatments have shown that retinoic acid and Fgf signaling, starting from E7.5, are required to define the size of the heart field (113) at the expense of limb precursors (104, 142), and later, at E9.5, to subdivide the heart field into an anterior and posterior domain, expressing the transcription factors Tbx1 and Tbx5, respectively, and providing cells to the arterial and venous poles of the heart, respectively (27).

The functional cardiac segments form sequentially along the axis of the cardiac tube—from the venous pole to the arterial pole, the left/right atria, the atrioventricular canal, the left ventricle, the right ventricle, and the outflow tract. The heart tube primordium, which is composed mainly of the left ventricle (149), elongates by incorporation of cardiac precursor cells at the venous and arterial poles. The identities of cardiac segments are progressively defined anatomically, as well as by the expression of transcription factors, such as *Nr2f2* in the atria, *Tbx2/3* in the atrioventricular canal, *Irx4* in the ventricles, or the expression of specific sarcomeric genes, such as *Myl2* and *Myl7* in the ventricles and atria, respectively. Single-cell transcriptomics have provided a more extensive profiling of cardiac regions (75), but mouse mutant analyses are necessary to demonstrate gene requirements for cardiac cell patterning.

Perturbations in heart patterning might be expected to impair the development of the left ventricle, a first lineage derivative—for example, in hypoplastic left heart syndrome (HLHS). This complex CHD has been recently modeled in the mouse by the double inactivation of *Sap130* and *Pcdba9*, which are involved in the chromatin-remodeling complex and cell adhesion, respectively (81). However, whether these genes play a role in heart patterning remains poorly understood. The contribution of the second heart field to both the arterial and venous poles of the heart is consistent with the association of conotruncal defects with anomalous pulmonary venous connections (10). Impairment of left/right patterning leads to heterotaxy, as shown in the mouse (114, 128). Human pathogenic variations in the *Mmp21*, *Zic3*, *Cfap52/54*, *Npbp4*, *Acvr2b*, *Cfc1*, *Foxb1*, *Gdf1*, *Lefty2*, or *Nodal* genes, which are required for the formation and function of the left/right organizer, are associated with the heterotaxy syndrome (44).

3.2. Alignment of Cardiac Segments

When the heart tube forms, the right ventricle is cranial (or superior; see E8.5f in **Figure 4**) to the left ventricle, whereas the atria are positioned on the left and right sides. In addition, the inflow and outflow tracts are continuous with the left and right ventricles, respectively (**Figure 3**). Thus, considerable morphogenetic movement is required to align cardiac chambers in the definitive configuration and bisect the heart into distinct blood flows, including heart looping, rotation of the outflow tract, pole convergence, wedging of the aorta, and rightward expansion of the atrioventricular canal.

The first step is heart looping, during which the cardiac tube acquires a helical shape. It occurs at mouse E8.5 (70) and at human CS9–11, at approximately 20–24 days of pregnancy (123). The loop shape has been proposed to provide a functional advantage, by increasing pumping efficiency and reducing retrograde flow before the formation of valves (47). Heart looping is also crucial to reposition the right ventricle from a cranial to a right position relative to the left ventricle. Early embryologists focused on the direction of the heart loop (28); thus, heart looping has been classically described as rightward (in a normal condition) or leftward (in laterality defects). Discovery of the mechanism of symmetry breaking in the left/right organizer, the node (118), has further supported the binary description of heart looping as a readout of the symmetry-breaking event and the resulting left-sided Nodal signaling. In this context, the positions of the ventricles after birth in the clinical nomenclature are described as D-loop or L-loop (139), although the relationship between the orientation of the embryonic loop of the heart tube and the positions of the ventricles after birth has never been demonstrated experimentally.

Laterality defects cannot be described solely in terms of inverted asymmetry (*situs inversus*) or abnormal symmetry (*isomerism*), as compared with normal asymmetry (*situs solitus*). In fact, heterotaxy is equivalent to *situs ambiguus*, meaning that left anomalies can be associated with right anomalies between different organs or between different heart segments. Furthermore, these

associations are not stereotyped, and the clinical picture of heterotaxy is highly variable. Looking at a single structure, such as the atria, one can see that the asymmetry parameters of the anatomy of the appendages and of the connection of the inferior caval vein are not always concordant (133). This lack of concordance is the basis of debates on the nomenclature of heterotaxy for the qualification of isomerism, i.e., bilateral symmetry (56), and shows that summarizing left/right asymmetry by a single symmetry-breaking event in the left/right organizer is not sufficient to understand laterality defects.

The heart loop has a 3D shape, a helix, which requires more parameters to describe its geometry than just its direction. To understand the mechanism of heart looping, 3D reconstructions of the dynamic shape changes and computer simulations have been performed [see video 2 in Reference 70 (<https://doi.org/10.7554/eLife.28951.013>)]. These are compatible with a buckling mechanism of heart looping (70, 109): The heart tube is physically deformed when it grows longitudinally, while the distance between the poles is fixed. The random deformations of buckling are biased by left/right asymmetries, to generate a helical shape of reproducible configuration. Quantitative analyses of the 3D shape and cell-labeling experiments have uncovered two sequential left/right asymmetries at the heart tube poles: A rotation of the arterial pole at E8.5f is followed by asymmetric cell incorporation at the venous pole at E8.5g (70). These asymmetries are not only sequential but also opposite (a rightward deformation at the arterial pole, and a leftward deformation at the venous pole), demonstrating that left/right asymmetry is not a single event.

Signaling by the left determinant *Nodal* does not interfere with the buckling mechanism; rather, it is essential for the amplification and coordination of left/right asymmetries at the heart tube poles (32). Thus, *Nodal* is necessary not only to control the direction of the heart loop (normally rightward) but also to shape the loop. In keeping with this finding, mice and patients with *Nodal* pathogenic variants do not display situs inversus; instead, they exhibit complex CHDs, including transposition of the great arteries (TGA), DORV, and atrioventricular septal defects (AVSDs) (96, 32). In the absence of *Nodal* in the mouse, four categories of embryonic heart loop shapes are produced, with the right ventricle cranial to the left, and in all possible lateral configurations (right/left ventricle positioned on the right/right, left/left, left/right, or right/left sides, respectively) (Figure 5). Further highlighting the role of *Nodal* in shaping, not just orienting, the heart loop, the leftward loop is not a mirror image of the control situation. This result may explain why situs inversus totalis (incidence 3/100,000) is not always a simple mirror image of the normal body plan, but can be associated with anomalies in the heart, spleen, and intestinal rotation (77). Another parameter of heart looping comes from mechanical constraints dorsally, when the heart tube is attached to the dorsal pericardial wall by the dorsal mesocardium. This tissue breaks down during heart looping, under the control of Sonic hedgehog (Shh) signaling (70).

Taking into account these few parameters (buckling, left/right asymmetries, and dorsal mesocardium breakdown), computer simulations can predict a range of heart loop shapes, some of which reproduce variations detected in mutant hearts [see figure 7 in Reference 70 (<https://doi.org/10.7554/eLife.28951.014>)]. This indicates that heart looping is a more complex process than initially thought, leading not only to leftward/rightward loops but also to specific configurations of cardiac chamber positions. The previous focus on the symmetry-breaking event as a binary decision (left or right) has masked the dynamics of left/right patterning. The clinical variability of heterotaxy may relate to the facts that left/right asymmetry is regulated independently at different levels and that asymmetry factors regulate different processes, including the initiation of the asymmetry, the fold difference between the left and right, and the laterality of the difference, i.e., whether a left determinant is localized on the anatomical right or left side. Abnormal alignment of cardiac chambers is a feature of 20% of CHDs, raising the possibility that

TGA: transposition of the great arteries

AVSD: atrioventricular septal defect

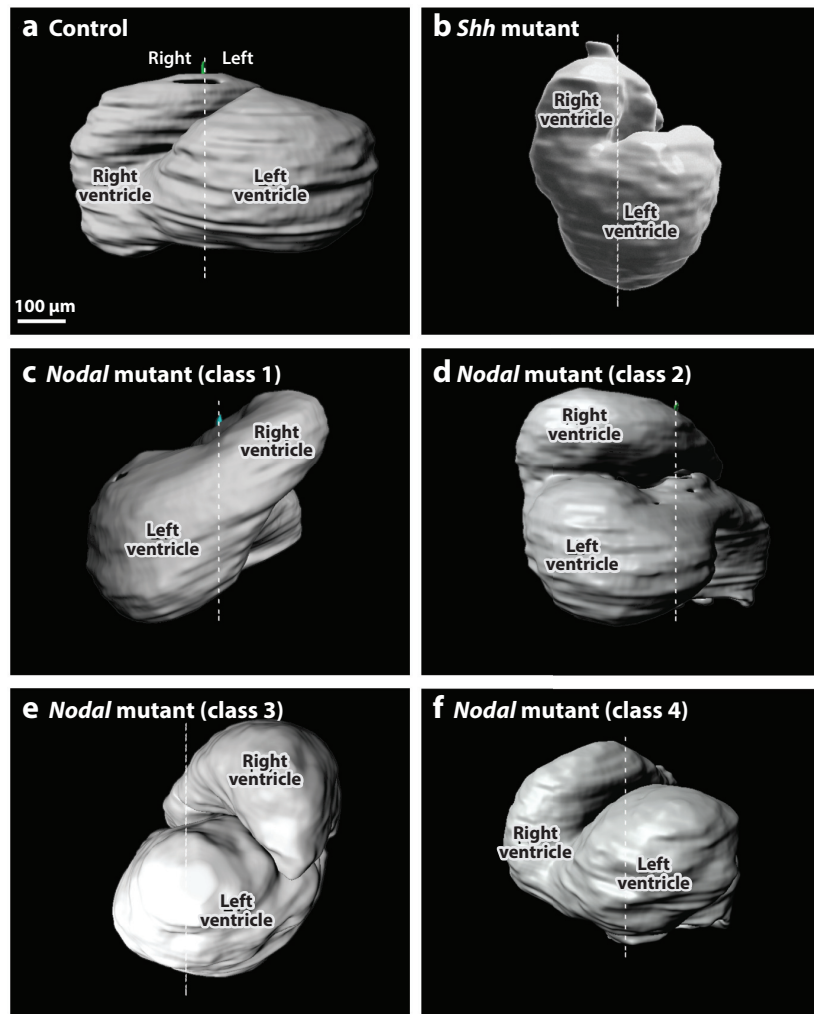


Figure 5

The diversity of heart loop shapes, showing 3D reconstructions of (a) the heart loop at E9.5 in wild-type mice, along with abnormal heart loops in (b) *Sbb*^{-/-} and (c-f) *Nodal*^{flax/mul};*Hoxb1*^{Cre/+} mutants. The white dotted line indicates the midline of the embryo, in a ventral view. Abbreviation: E, embryonic day. For more details, see References 32 and 70. We thank A. Desgrange for the 3D reconstructions.

looping anomalies lead not only to heterotaxy but also to complex malformations such as TGA, DORV, AVSDs, congenitally corrected TGA, supero-inferior ventricles, and crisscross hearts.

The rightward rotation of the arterial pole seen in the early embryo at E8.5 (70) continues until the fetal stages, as detected by cell labeling and transgenic markers (9, 131). This rotation underlies the spiraling of the great arteries. In mutants for the Nodal target *Pitx2*, TGA and DORV are associated with abnormal patterning of the transgene, indicative of abnormal rotation. The absence of spiraling of the great arteries, usually associated with an abnormal position of the aorta remaining on the right, above the right ventricle, is an anatomical marker of defective outflow tract rotation. CHDs resulting from an abnormal alignment of the great arteries with the ventricles (outflow tract defects) include conotruncal defects, TGA, and DORV (Figure 1). DORV is a type

of ventriculo-arterial connection in which both great arteries arise predominantly from the morphologically right ventricle (38). However, different phenotypes exist according to the position of the VSD relative to the great vessels, with specific impacts on blood circulation: committed to the aorta (outlet subaortic VSD), committed to the pulmonary artery (outlet subpulmonary VSD), committed to both great arteries (outlet doubly committed VSD), or noncommitted (74). The commitment of the VSD to the great vessels depends on the position of the outlet septum relative to the septal band on the right ventricular septal surface (5): posterior in DORV with a subpulmonary VSD (developmentally related to TGA) or anterior in DORV with a subaortic VSD (developmentally related to outlet VSDs or tetralogy of Fallot).

The venous pole—which is initially, at E8.5, the caudal aspect of the heart tube—converges to the cranial arterial pole after looping, between E9.5 and E10.5, thus lying dorsal to it (109). The mechanism controlling the distance between the poles is currently unclear; a caudal movement of the outflow tract relative to the pharyngeal region has been observed, as the arch arteries open sequentially (141), and an association with the cervical flexure has been proposed (87). The outflow tract forms initially on the right side of the heart, continuous with the right but not the left ventricle, whereas the atrioventricular canal forms on the left, continuous with the left but not the right ventricle. At birth, both structures are medial, lying above one another, and have been connected to each ventricle, thus implying a displacement (135). Advanced 3D imaging of the heart anatomy has shown that a leftward shift of the aortic root occurs just before birth in the mouse, between E16.5 and E18.5 (97), often referred to as wedging of the aortic valve between the atrioventricular valves (11) (E14.5 in **Figure 3a**). In humans, wedging is completed at the end of the embryonic period (CS23). By contrast, the atrioventricular canal is displaced rightward from the mouse E11 and human CS15 stages, thus allowing a direct connection between the right atrium and the right ventricle. The underlying mechanism potentially involves growth by enlargement of the atrioventricular canal and/or remodeling of the inner curvature, as tracked by clonal analysis and genetic markers, respectively (69, 92, 143). Incomplete alignment between the atria and the ventricles might be associated with a lack of ventricular growth or an absent or anomalous development of the right atrioventricular junction. This is the case in double-inlet ventricle, tricuspid or mitral atresia, and ventricular hypoplasia.

3.3. Heart Septation

When the cardiac segments are correctly aligned, independent growth of septa bisects the ventricles, the atria, and the outflow tract (**Figure 3**).

Ventricular septation begins at mouse E10.5 and at human CS14, at approximately 31–35 days of pregnancy (6, 37, 121), through the outgrowth of a muscular ridge at the level of the sulcus between the left and right ventricles. Ventricular septation has been proposed to depend on the coalescence of trabeculations, based on cell labeling in the chick model (45) and anatomical observations (13). This idea is further supported by the phenotypic association in mouse models of muscular VSDs with trabecular compaction defects (132). Lineage analyses have shown that the ventricular septum receives a contribution from both the right and left ventricles (37). The septum forms at the boundary of gene expression, such as that of the transcription factors *Tbx5* and *Tbx18* (19, 37); shifts in the *Tbx5* expression boundary result in septation abnormalities (64). This is in keeping with the ventricular septation defects associated with human pathogenic variation in *Tbx5* in Holt–Oram syndrome (76). Septation is completed by fusion with mesenchymal cells of the outflow cushions and the atrioventricular cushions, thus composing the membranous part of the interventricular septum at mouse E13.5 or human CS22 (29, 66, 97). The clinical nomenclature of VSDs, based on the locations of the defects in the ventricular septum, reflects

the embryological sequence and tissue contribution: Anomalies in the formation of the muscular ridge lead to muscular VSDs, failure to remodel the primary atrioventricular communication by the rightward expansion of the atrioventricular canal results in inlet VSDs, failure to remodel the ventriculo-arterial communication by rotation and wedging of the aorta results in outlet VSDs, and failure to complete septation by the membranous septum derived from the atrioventricular cushions results in central perimembranous VSDs (7) (**Figure 2**).

Atrial septation, similar to ventricular septation, is initiated at mouse E10.5 or at human CS14, at approximately 31–35 days of pregnancy (66), by an outgrowth in the roof of the left atrium. The left origin of this primary atrial septum is shown by a transgenic marker that reports signaling by the left determinant *Nodal* (39). In *Nodal* mouse mutants, atrial septation is consistently absent, in association with right atrial isomerism (32). At the leading edge of the muscular primary atrial septum, an endocardial thickening, referred to as the mesenchymal cap (8), progresses until fusion with the atrioventricular cushions. A secondary nonmuscular contribution to atrial septation is from the so-called dorsal mesenchymal protrusion, which is derived not from the endocardium but from the *Isl1*-positive second heart field, to which the heart is dorsally connected (124). Complete fusion of the dorsal mesenchymal protrusion, mesenchymal cap, and atrioventricular cushions results in the closure of the primary atrial foramen. The secondary atrial foramen forms by fenestrations of the primary atrial septum along its attachment to the dorsal roof of the atrium (98). By E14.5, mesenchymal components of the atrial septum are muscularized, and another muscular ridge forms by invagination of the roof of the right atrium, which is a tertiary component to atrial septation (the superior interatrial fold, or so-called septum secundum) (98). This muscular ridge fuses to the primary atrial septum after birth, closing the oval foramen.

Signaling by *Shh* is essential for atrial septation. *Shh* is secreted by the pulmonary endoderm and received, between E8 and E10, by cells in the posterior second heart field, traced by the expression of the *Shh* target *Gli1* (50). These cells migrate through the dorsal mesocardium to the primary atrial septum and dorsal mesenchymal protrusion. When the cells are rendered unresponsive to *Shh*, they populate the atrial free wall rather than the septum. *Gli1* genetically interacts with *Tbx5* in the second heart field to coactivate downstream targets, including the transcription factors *Osr1* and *Foxf1*, and promotes the proliferation and specification of atrial septum progenitors (51, 152). Human pathogenic variations in *Tbx5* in Holt–Oram syndrome are associated with atrial septal defects (ASDs). The majority of ASDs correspond to excessive or ectopic fenestrations in the primary atrial septum (defects in the oval fossa, also called secundum ASDs). Rarer forms include abnormal communications between right pulmonary veins and caval veins (sinus venosus defects) and partial or complete absence of the wall of the coronary sinus (coronary sinus defects). In AVSDs, there is a common atrioventricular junction, including various degrees of inlet VSD, persistence of the primary atrial foramen (also called primum ASDs), and a common atrioventricular valve with one or two orifices. AVSDs result predominantly from a deficiency of the dorsal mesenchymal protrusion, which is itself derived from the posterior second heart field (15, 17).

In the outflow tract, septation begins at mouse E9.5 or at human CS13, at approximately 28–32 days of pregnancy (122), with the formation of endocardial cushions, which correspond to a bulge of extracellular matrix colonized by mesenchymal cells (90). The overlying myocardium, which is prepatterned by the expression of transcription factors such as *Tbx2* (46), secretes cardiac jelly (117) and promotes the epithelial–mesenchymal transition of endocardial cells via *TGF β* (115) and *Bmp* (62, 79) paracrine signaling. When they form, outflow cushions have a spiral arrangement (65, 97), which reflects the rightward rotation of the outflow tract. While the outflow tract myocardium grows by addition of cells from the second heart field (60), outflow tract cushions are invaded from E9.5 by another type of mesenchymal cell, derived from the neural crest, as evidenced by grafts and genetic tracing (57). Condensation of this outflow mesenchyme

triggers the fusion of cushions and the rupture of the endocardium in between. This process is initiated around E11.5 in the aortic sac and progresses in the truncus or distal outflow tract, toward the conus or proximal outflow tract. This forming aorticopulmonary septum, which has a spiral shape, separates the trunks of the aorta and pulmonary artery distally and the outlets of the left and right ventricles proximally (outlet septum). The distal septum differentiates into smooth muscle (57), whereas the proximal septum of the outflow tract is secondarily myocardialized (145).

Ablation or impaired migration of cardiac neural crest cells impairs outflow tract septation, leading to CAT, DORV, outlet VSDs, and abnormal patterning of the aortic arch arteries (24, 63) (**Figure 1**). Bmp signaling, secreted by the myocardium and sensed by the cardiac neural crest, is essential for outflow tract septation, by orchestrating the progressive zipper-like septum formation in time and space. Reducing Bmp signaling by depletion of either Bmp4 or the receptor Bmpr1a or by forced expression of the antagonist Smad7 impairs cushion formation and septation of the outflow tract (79, 125, 129). Conversely, enhancing Bmp signaling by depletion of the inhibitor Ctdnep1 in the neural crest cells leads to premature mesenchyme condensation and septation of the outflow tract, as well as pulmonary artery stenosis (26). One effector of Bmp signaling is the secreted factor Sema3c (26, 79). Cardiac neural crest cells transit through the branchial arches, where they surround a core of other mesodermal cells from the anterior second heart field. These cell types interact so that disruption of cardiac neural crest cell migration has secondary consequences for the proliferation of second heart field cells and their differentiation into cardiomyocytes, thus shortening the outflow tract and preventing completion of heart looping (140, 146). Reciprocally, inactivation of *Tbx1*, which is expressed in the second heart field but not in cardiac neural crest cells, impairs outflow tract septation and cardiac neural crest cell migration (151). *Tbx1* is the major causative gene of 22q11.2 deletion syndrome (also known as DiGeorge or velo-cardio-facial syndrome) (93), which presents a spectrum of conotruncal malformations, including CAT, DORV with a subaortic or juxta-arterial outlet VSD, tetralogy of Fallot, outlet malalignment VSDs, and IAA type B. Another important signaling for outflow tract septation is Shh, which is secreted by the pharyngeal endoderm and received, between E8 and E10, by progenitors of the anterior second heart field, stimulating their incorporation into the subpulmonary myocardium (50), as well promoting cardiac neural crest cell survival (42).

The circuitry underlying the double blood circulation is thus established during fetal life. However, before the lungs become functional at birth, bypasses are present between the atria (oval foramen) and between the great arteries (arterial duct). Septal defects are the most frequent forms of CHDs: 35–50% are VSDs, 20% are outflow tract defects, and 6–15% are ASDs (61, 82).

3.4. Valvulogenesis

Important for the unidirectional blood flow is the formation of valves at the entrance and exit of the ventricles. Valvulogenesis begins with the formation of endocardial cushions in the outflow tract and atrioventricular canal. Whereas the main (septal) cushions required for septation are already detectable at E9.5, additional cushions—referred to as intercalated cushions in the outflow tract and lateral cushions in the atrioventricular canal—emerge at mouse E11.5 (30, 35, 95, 97) or at human CS16, at approximately 38–41 days of pregnancy (121). The main outflow tract cushions give rise to the left and right valve leaflets of each semilunar valves, whereas the intercalated cushions form the anterior pulmonary and posterior aortic leaflets (65) (E14.5 in **Figure 3a**). Similarly, the main (superior/inferior) atrioventricular cushions contribute to the anterior mitral leaflet and the septal tricuspid leaflet (30), whereas the lateral cushions become the posterior mitral and the anterior and postero-inferior tricuspid leaflets. Genetic tracing experiments have uncovered the origin of valve cells. Valves are derived predominantly from the endocardium (30, 78). The

epicardium contributes valvular interstitial cells to the lateral atrioventricular cushions (144). The aortic and pulmonary semilunar valves receive a contribution from cardiac neural crest cells in the left and right leaflets (57, 106), whereas the posterior aortic and anterior pulmonary valve leaflets, corresponding to the intercalated cushions, are colonized by second heart field cells (35, 95).

Similar to the mechanism in the outflow tract, the formation of atrioventricular cushions depends on Bmp and TGF β signaling (18, 41, 85). In addition, Notch1 signaling in the endocardium is required for the initiation of the epithelial–mesenchymal transition and interacts with Bmp2 in the overlying myocardium (84). Ablation or impaired migration of cardiac neural crest cells leads to aortic valve defects (106, 111).

The septal and postero-inferior leaflets of the tricuspid valve detach sequentially from the myocardium through a process of delamination starting at human CS20, at approximately 8 weeks of pregnancy (59, 68). This is also the case for the mural leaflet of the mitral valve, but not for the semilunar valves. Valve primordia elongate from the cushions, by cell proliferation and secretion of extracellular matrix (48), under the positive control of Bmp and Fgf signaling and the negative control of Egf and Notch (22, 86, 126). The tendinous cords, tethering atrioventricular valves to the ventricular papillary muscles and the fibrous annulus, corresponding to the valve insertion at the atrioventricular junction, develop at fetal stages and are derivatives of the endocardium (30, 107). The valve primordia are remodeled postnatally into stratified leaflets, composed of three layers of extracellular matrix (fibrosa, spongiosa, and ventricularis/atrialis) interspaced with valve interstitial cells, and covered by valve endothelial cells.

Valve diseases are most commonly found in the mitral and aortic valves, i.e., in the systemic circulation (49). The most frequent congenital valve anomalies include bicuspid aortic valve, in which two leaflets form instead of three, and myxomatous mitral valve disease, in which the extracellular matrix is disorganized, leading to valve thickening, deformation, and regurgitation. In several cases, valve diseases are associated with the reactivation of developmental pathways (67). An example of this is mitral valve prolapse associated with Marfan syndrome, a disease caused by mutations in a component of the extracellular matrix *Fbn1*, which limits TGF β signaling (103). Another example is aortic valve disease associated with *Notch1* mutations (40). Since the main outflow and atrioventricular cushions contribute to both septation and valve formation, valve defects in patients are commonly associated with VSDs, DORV, and multilevel left heart obstruction, including aortic coarctation. In the physiologically right heart, tricuspid anomalies are severe for their hemodynamic consequences during fetal life and are the leading cause of fetal demise. Ebstein anomaly of the tricuspid valve is defined by a lack of delamination of the septal and/or inferior leaflets associated in the most anatomically complex forms with abnormal development of the subvalvar apparatus (tendinous cords and papillary muscles) of the anterior leaflet. Dysplastic tricuspid valve displays normally delaminated but dysplastic leaflets with short or absent tendinous cords. Severe tricuspid regurgitation potentially caused by these tricuspid abnormalities can lead to progressive hypoplasia or even closure of the pulmonary valve (21). This illustrates the major role of fetal hemodynamics in the detrimental progression of left and right heart valvar obstructive disease. Similarly, any reduction in blood flow through the left ventricle can lead to abnormal development of the mitral valve, the left ventricle, the aortic valve, and the aortic arch (2).

4. STATE OF THE ART AND FUTURE CHALLENGES

In the last few decades, refinement of the classification of CHDs and advances in the experimental elucidation of developmental mechanisms of heart formation and malformation have changed our understanding of CHDs and greatly improved patient management. However, several challenges lie ahead to explain the phenotypic diversity of structural CHDs, uncover their genetic and

nongenetic origins, and characterize associated deficiencies that can continue to affect patients after surgical repair.

4.1. Mechanisms Leading to Congenital Heart Defects

As seen in the previous sections, from the parallel increase in anatomical observations and experimental results in the animal models, the mechanisms of conotruncal defects, AVSDs, ASDs, VSDs, and valve defects have been well explored. More complex CHDs are currently unresolved, including congenitally corrected TGA, crisscross hearts, anomalous pulmonary venous connections, and pulmonary atresia with intact ventricular septum. The etiology of functionally univentricular hearts also remains poorly understood.

As shown in the case of conotruncal defects (**Figure 5**), CHDs can form a spectrum. This is the case when variations in the same genetic pathway or same developmental process result in distinct but related CHDs, because of common features, such as the outlet VSD in the case of conotruncal defects. The numbers and extent of the phenotypic spectra of structural CHDs are currently unknown. In the case of the heterotaxy syndrome, which has been clearly associated with anomalies in the formation and function of the left/right organizer (44, 114, 128), the origin of the phenotypic variability of associated CHDs remains poorly understood. In the mouse, a single-gene inactivation is associated with a spectrum of defects, some of which have partial penetrance (32, 33). This points to the need to uncover the mechanisms of asymmetric organogenesis beyond the left/right bias provided by the left/right organizer. In particular, the mechanisms of outflow tract rotation, convergence of the arterial and venous poles, and wedging of the aortic valve remain unclear. In addition, for any single gene, the spatiotemporal context of gene function has to be dissected. This is illustrated by Notch signaling, which depends on paralog ligands and receptors and plays sequential roles in different embryological processes, including left/right patterning, myocardium differentiation and trabeculation, valve formation, and coronary development (86).

In reverse, close variations of a specific CHD can correspond to different embryological mechanisms. This is illustrated by DORV, an anomaly of the outflow tract, which has a range of phenotypic variations. DORV with a subaortic or doubly committed juxta-arterial outlet VSD is considered part of the anatomical spectrum of cardiac neural crest and anterior second heart field defects (conotruncal defects), because of the anatomical similarities with tetralogy of Fallot and similar orientation of the coronary orifices (53). DORV is also frequently encountered in heterotaxy, especially in association with AVSDs. Genetic mutations in *CFC1*, *NODAL*, or *ZIC3* are found in humans and mice in association with heterotaxy, DORV, and TGA, indicating that some isolated forms of TGA and DORV could be part of the spectrum of laterality defects (43). A recent study has shown that DORV with a subpulmonary outlet VSD is closely related to TGA in terms of coronary patterning (138) or the outflow tract type of cleft mitral valve. Finally, DORV with noncommitted VSD (inlet or muscular VSD) involves an earlier stage of interventricular septation and is associated with more severe CHDs (hypoplastic ventricle or heterotaxy). This suggests an earlier embryological anomaly, in heart patterning, rather than in outflow tract formation. The mechanisms by which anomalies in left/right patterning or in the deployment of the cardiac neural crest/anterior second heart field lead to distinct types of VSDs remain an open question. In the future, it will be important to distinguish the types of VSDs associated with DORV when phenotyping mouse models.

The same anatomical CHD can result from distinct processes. This is best shown for AVSDs. Hierarchical clustering analysis of the co-occurrence of specific CHDs in families has highlighted two types of AVSD—isolated cases and cases associated with CHDs in the setting of heterotaxy syndromes (36)—suggesting distinct genetic mechanisms. Mouse studies of AVSDs associated

with variants of ciliary genes are consistent with this clustering (20). During development, cilia are required for two distinct processes: primary and motile cilia for left/right symmetry breaking in the left/right organizer, and primary cilia for Hedgehog (Hh) signaling in the posterior second heart field. Genetic mutations that affect cilium motility and thus left/right patterning, but not the second heart field, were found in AVSD cases associated with heterotaxy. Mutations in ciliary genes found in isolated AVSD cases, without heterotaxy, affect the second heart field but not left/right patterning. Finally, a group of AVSDs irrespective of heterotaxy are associated with variants of ciliary genes that affect both the second heart field and left/right patterning (20).

Confusions in the field of CHDs have arisen from a lack of interdisciplinarity. Although anatomical correlations can lead to relevant hypotheses, they are not sufficient to draw conclusions about causality, which must be experimentally established in animal models using multiscale (molecular, cellular, tissue, and organ) analyses. Conversely, superficial and nonquantitative phenotyping of CHDs in animal and genetic studies prevents the integration of mechanistic data into the classification of CHDs. In the future, the general use of ICD-11 anatomical criteria will be essential for sharing a common language, comparing data sets, and thus combining knowledge across disciplines. Resolution of the fine anatomical details is best provided by 3D imaging, in which different section planes can be used to diagnose distinct anatomical features, compared with traditional histological sections. In the mouse, micro-MRI, micro-CT, high-resolution episcopic microscopy, and episcopic confocal microscopy are now available (33, 80, 97) and will be applicable to postmortem human specimens.

4.2. Genetics of Structural Congenital Heart Defects

Compared with syndromic diseases with CHDs (112) and most cardiomyopathies (147), the genetic origin of nonsyndromic structural CHDs is more complex. With the development of next-generation sequencing and bioinformatic and statistical analyses, the number of rare sequence variants identified in children with CHDs is exploding, with an estimated 392–440 genes with de novo mutations associated with CHDs (52, 58). However, in most patients, a single-gene mutation can explain neither their phenotype nor the large variability of the phenotypes for a given malformation. Thus, establishing the disease causality of a specific variant remains a challenge. Most CHDs (97.8%) are sporadic, i.e., with no affected first-degree relatives (108), which might suggest a role for de novo mutations (150) in accordance with an increased paternal age at conception. However, de novo mutations were found in only 10% of CHDs, and single-gene variants were found in 3.5% (150). The increased incidence of CHDs in populations with high levels of consanguinity also suggests a role for recessive genetic contributions (116). Inherited variants are more frequently associated with nonsyndromic CHDs, compared with syndromic cases (119); 2% of CHD cases were found to be attributable to inherited autosomal recessive variants (58).

Rates of recurrence among first-degree relatives of patients with CHDs suggest an overall risk of 5–10% for any CHD when either one parent or more than two siblings are affected, or approximately 3% when one child is affected (112). This suggests that the majority of CHDs have a multifactorial origin. In most families, only one person has a CHD; however, the risk of CHDs increases for children born into families already affected. Heterotaxy and right ventricular outflow tract obstructive lesions display the highest relative risk of recurrence (79% and 48.6%, respectively), followed by AVSDs (24.3%), left ventricular outflow tract obstructive lesions (12.9%), and conotruncal defects (11.7%) (108). Analysis of the recurrence of distinct CHDs in the same family indicates that there are common genetic pathways underlying a spectrum of CHDs. Using the IPCCC codes and a hierarchical clustering of the log-odds ratio, researchers have identified patterns of familial co-occurrence of CHDs, highlighting 10 distinct groups. Several of these groups

are consistent with known developmental processes, corresponding to ASDs, AVSDs, right ventricular outflow tract obstruction, left ventricular outflow tract obstruction, outflow tract defects, and left/right anomalies, and some new groups have been identified (36).

There is thus accumulating evidence of a genetic origin of structural CHDs. The incomplete segregation of familial CHDs could be attributable to incomplete penetrance, oligogenic origins of CHDs, or both (150). This has been demonstrated for HLHS. Based on a forward genetic screen in the mouse using the clinical nomenclature, 330 genetic variants associated with HLHS have been identified. A combination of two variants is sufficient to generate HLHS with a 26% penetrance among a spectrum of defects, including bicuspid aortic valve, isolated hypoplastic left ventricle or aorta, and DORV (81). In the future, more complex modes of inheritance will have to be considered, wherein, for example, a heterozygous mutation requires a modifier mutation or the absence of a protective variant to manifest as disease, or a convergence of hypomorphic mutations in several components of a single pathway must reach a threshold to manifest as disease. Another approach is a gene burden system, combining a series of genomic alterations of different weights, some inherited, some *de novo*. In either case, the contribution of variants in noncoding DNA remains underexplored. To conduct these complex genetic analyses, the ongoing sharing and harmonization of data in large-scale consortia will be key, associated with precise and standardized phenotype annotations, the development of algorithms to extract information from big data, and the development of tailored animal models to test specific genetic hypotheses.

4.3. Gene–Environment Interactions

In addition to genetic factors, the role of epigenetic mechanisms—chromatin remodeling, DNA methylation, and histone modifications—in CHDs is emerging (112). The list of gene variants associated with CHDs contains many chromatin-modifying genes (52, 150). Epigenetic factors influence the regulation of transcription factors, like *Tbx1*, which is affected by 22q11 microdeletion, and could explain the variability of phenotypes in DiGeorge syndrome (99). CHDs are observed in cohesinopathies, in which the cohesin protein complex is affected, which disrupts 3D DNA loops that control gene regulation (99). This is the case for Cornelia de Lange syndrome, which is associated with CHDs such as tetralogy of Fallot, septal defects, and pulmonary stenosis. Since many of the proteins mediating epigenetic regulations are widely expressed, how they play a role in specific CHDs remains unknown.

Environmental factors can also interact with genetic factors and partly explain the variable penetrance and expressivity of genetic variants. For example, gestational hypoxia has been recognized as a triggering mechanism of CHDs in genetically susceptible mouse embryos (100). In these mice, hypoxia disrupted *Fgf* signaling in the second heart field, along with important transcription factors involved in heart development, such as *Tbx1*, *Tbx5*, and *Nkx2–5*. CHD penetrance increased as oxygen levels decreased, whereas the same genetically modified mice did not exhibit any CHDs in the absence of hypoxia. Some teratogens, such as tobacco, as well as high altitude and obesity of the mother, can induce CHDs similarly to hypoxia (23, 127, 148). CHDs have been associated with other environment factors, including drugs and toxic products (anticonvulsants, antidepressants, alcohol, and isotretinoin), as well as diabetes in the mother (100). The impact of pesticides in CHDs awaits a comprehensive analysis.

Hemodynamics also plays a major role during fetal life as a modifier of an initial perturbation of normal cardiac development in the embryo, especially in left and right ventricular obstructive lesions (2). Hemodynamics could also intervene much earlier in cardiac development, acting directly on cardiomyocytes and endocardial cells in endocardial cushions and through mechanosensors and mechanotransducers, including primary cilia (25). A recent experimental study in chick embryos,

using different degrees of outflow tract banding or ligation of the right vitelline vein early in cardiac development, demonstrated that the type of malformation obtained (VSDs, DORV, tetralogy of Fallot, or anomalies of the pharyngeal arches) varies with the degree of banding and between the banding and vein ligation groups. The vein ligation group exhibited isolated malformations of the pharyngeal arches with hypoplastic aorta, which were distinct from the malformations of the aortic arches associated with DORV or tetralogy of Fallot that were observed after banding of the outflow tract. The degree of hemodynamic impairment at the heart tube stage is thus predictive of distinct CHD phenotypes, which could be due at least in part to perturbations of the epithelial–mesenchymal transition in the outflow tract cushions (94). Genetic and hemodynamic factors are thus tightly intertwined.

4.4. Association of Congenital Heart Defects with Other Organ Defects

Among children with CHDs, 13% have associated extracardiac malformations, compared with 7% in the general population (150). Many of these anomalies are found in the setting of syndromes, including heterotaxy and chromosomal abnormalities, thus pointing to a common genetic origin.

As the vast majority of neonates with CHDs survive well beyond infancy, neurodevelopment constitutes a major issue. Neurodevelopmental disabilities affect 10% of children with mild CHDs and up to 50% of those with severe CHDs that required surgical repair during infancy (150). White matter alterations and immaturity are commonly associated with CHDs (101). The prevalence of attention deficit and/or hyperactive disorder is increased two- to fourfold in children with CHDs compared with the general population (89, 134). Children with ASDs and VSDs are at a higher risk of developing autism (120). In HLHS, the incidence of neurodevelopmental disabilities reaches 70% (89). Some CHDs, such as HLHS, may have a common genetic or epigenetic cause with abnormal brain development. A candidate gene is *RBFox2*, which encodes a regulator of RNA splicing (52). For a long time, most of the neurodevelopmental disabilities were thought to result from oxygenation changes during cardiac bypass surgery. However, there is increasing evidence that neurodevelopmental impairments in children with CHDs are also secondary to impaired cardiovascular physiology in the fetus (110). In addition, fetal cerebral blood flow is altered in fetuses with HLHS, suggesting a role of fetal hemodynamics in the neurological outcome of children with CHDs (101).

4.5. Adults with Congenital Heart Defects

Following the tremendous advances in the surgical repair of CHDs in children during the last half century, along with advances in prenatal and postnatal diagnosis and in medical management of neonates, including the use of prostaglandin E1 to keep the arterial duct open, the epidemiology of CHDs in developed countries has changed considerably. Although CHDs remain the first cause of neonatal mortality, approximately 30% of children born with a CHD require surgical or transcatheter intervention in the first year of life, and the survival rate is now above 90% (88). However, surgery has not solved all the deficiencies, which raises emerging problems for the long-term follow-up of patients: There is an increased burden of heart failure and arrhythmias in the adult population, and approximately 30% of adults operated on in childhood for a CHD will need reintervention (55).

5. CONCLUSIONS

With the enormous progress in clinical and basic research, most CHDs are no longer unavoidably fatal at birth. However, they are incompletely understood and remain a major medical issue. The

complexity of the genetic inheritance and phenotypic variability of CHDs is among the challenges to address, abandoning the overly simplistic association of one gene with one embryological process with one disease. With the advent of big data in omics and imaging and the development of analytic algorithms, heart development and CHDs can be investigated more quantitatively, taking into account the multiplicity of molecular pathways and their dynamic spatiotemporal context. Further deciphering CHDs will be possible only through close interactions among all the actors in the diagnosis, treatment, and physiopathology of CHDs, including pediatric cardiologists, congenital cardiac surgeons, radiologists, cardiac anatomists, fetopathologists, obstetricians, and basic scientists involved in the embryology, genetics, and epigenetics of CHDs, in epidemiology, and in the development of computational tools. The nomenclature and classifications of CHDs provide a standardized phenotyping to integrate knowledge across disciplines. Interdisciplinary interactions, in turn, are expected to refine the current classifications, to better identify families of CHDs with a shared mechanistic origin. Ultimately, close collaboration between clinicians and researchers is beneficial for all patients born with congenital cardiac malformations.

DISCLOSURE STATEMENT

The authors are not aware of any affiliations, memberships, funding, or financial holdings that might be perceived as affecting the objectivity of this review.

ACKNOWLEDGMENTS

We thank D. Rocancourt and G. André for schemes shown in **Figures 1** and **2**, respectively, and A. Desgrange for the 3D reconstructions shown in **Figure 5**. We thank S. Lyonnet for insightful discussions. Work in the Meilhac laboratory is supported by core funding from the Institut Pasteur and by state funding from the Agence Nationale de la Recherche under the “Investissements d’avenir” program (ANR-10-IAHU-01 and Inception program ANR-16-CONV-0005). S.M.M. is an INSERM research scientist.

LITERATURE CITED

1. Abbott M. 1936. Atlas of Congenital Cardiac Disease. *Can. Med. Assoc. J.* 34:194–95
2. Agnoletti G, Anecchino F, Preda L, Borghi A. 1999. Persistence of the left superior caval vein: Can it potentiate obstructive lesions of the left ventricle? *Cardiol. Young* 9:285–90
3. Anderson RH. 2017. Has the congenitally malformed heart changed its face? Journey from understanding morphology to surgical cure in congenital heart disease. *Circ. Res.* 120:901–3
4. Anderson RH, Becker AE, Freedom RM, Macartney FJ, Quero-Jimenez M, et al. 1984. Sequential segmental analysis of congenital heart disease. *Pediatr. Cardiol.* 5:281–87
5. Anderson RH, Becker AE, Wilcox BR, Macartney FJ, Wilkinson JL. 1983. Surgical anatomy of double-outlet right ventricle—a reappraisal. *Am. J. Cardiol.* 52:555–59
6. Anderson RH, Spicer DE, Brown NA, Mohun TJ. 2014. The development of septation in the four-chambered heart. *Anat. Rec.* 297:1414–29
7. Anderson RH, Spicer DE, Mohun TJ, Hikspoors JPJM, Lamers WH. 2019. Remodeling of the embryonic interventricular communication in regard to the description and classification of ventricular septal defects. *Anat. Rec.* 302:19–31
8. Arrechedera H, Alvarez M, Strauss M, Ayesta C. 1987. Origin of mesenchymal tissue in the septum primum: a structural and ultrastructural study. *J. Mol. Cell. Cardiol.* 19:641–51
9. Bajolle F, Zaffran S, Kelly RG, Hadchouel J, Bonnet D, et al. 2006. Rotation of the myocardial wall of the outflow tract is implicated in the normal positioning of the great arteries. *Circ. Res.* 98:421–28
10. Bajolle F, Zaffran S, Losay J, Ou P, Buckingham M, Bonnet D. 2009. Conotruncal defects associated with anomalous pulmonary venous connections. *Arch. Cardiovasc. Dis.* 102:105–10

11. Bartelings MM, Gittenberger-de Groot AC. 1989. The outflow tract of the heart—embryologic and morphologic correlations. *Int. J. Cardiol.* 22:289–300
12. Béland MJ, Franklin RC, Aiello VD, Houyel L, Weinberg PM, Anderson RH. 2018. Nomenclature and classification of cardiac defects. In *Pediatric and Congenital Cardiology, Cardiac Surgery and Intensive Care*, ed. EM da Cruz, D Ivy, V Hraska, J Jagers, pp. 1–23. London: Springer
13. Ben-Shachar G, Arcilla RA, Lucas RV, Manasek FJ. 1985. Ventricular trabeculations in the chick embryo heart and their contribution to ventricular and muscular septal development. *Circ. Res.* 57:759–66
14. Bernheim S, Meilhac SM. 2020. Mesoderm patterning by a dynamic gradient of retinoic acid signalling. *Philos. Trans. R. Soc. Lond. B* 375:20190556
15. Blom NA, Ottenkamp J, Wenink AGC, Gittenberger-de Groot AC. 2003. Deficiency of the vestibular spine in atrioventricular septal defects in human fetuses with down syndrome. *Am. J. Cardiol.* 91:180–84
16. Botto LD, Lin AE, Riehle-Colarusso T, Malik S, Correa A. 2007. Seeking causes: classifying and evaluating congenital heart defects in etiologic studies. *Birth Defects Res. A* 79:714–27
17. Briggs LE, Kakarla J, Wessels A. 2012. The pathogenesis of atrial and atrioventricular septal defects with special emphasis on the role of the dorsal mesenchymal protrusion. *Differentiation* 84:117–30
18. Brown CB, Boyer AS, Runyan RB, Barnett JV. 1999. Requirement of type III TGF- β receptor for endocardial cell transformation in the heart. *Science* 283:2080–82
19. Bruneau BG, Logan M, Davis N, Levi T, Tabin CJ, et al. 1999. Chamber-specific cardiac expression of Tbx5 and heart defects in Holt-Oram syndrome. *Dev. Biol.* 211:100–8
20. Burnicka-Turek O, Steimle JD, Huang W, Felker L, Kamp A, et al. 2016. Cilia gene mutations cause atrioventricular septal defects by multiple mechanisms. *Hum. Mol. Genet.* 25:3011–28
21. Celermajer DS, Bull C, Till JA, Cullen S, Vassilikos VP, et al. 1994. Ebstein's anomaly: presentation and outcome from fetus to adult. *J. Am. Coll. Cardiol.* 23:170–76
22. Chen B, Bronson RT, Klamann LD, Hampton TG, Wang JF, et al. 2000. Mice mutant for Egfr and Shp2 have defective cardiac semilunar valvulogenesis. *Nat. Genet.* 24:296–99
23. Chun H, Yue Y, Wang Y, Dawa Z, Zhen P, et al. 2019. High prevalence of congenital heart disease at high altitudes in Tibet. *Eur. J. Prev. Cardiol.* 26:756–59
24. Conway SJ, Henderson DJ, Copp AJ. 1997. Pax3 is required for cardiac neural crest migration in the mouse: evidence from the splotch (Sp2H) mutant. *Development* 124:505–14
25. Courchaine K, Rykiel G, Rugonyi S. 2018. Influence of blood flow on cardiac development. *Prog. Biophys. Mol. Biol.* 137:95–110
26. Darrigrand J-F, Valente M, Comai G, Martinez P, Petit M, et al. 2020. Dullard-mediated Smad1/5/8 inhibition controls mouse cardiac neural crest cells condensation and outflow tract septation. *eLife* 9:e50325
27. De Bono C, Thellier C, Bertrand N, Sturny R, Jullian E, et al. 2018. T-box genes and retinoic acid signaling regulate the segregation of arterial and venous pole progenitor cells in the murine second heart field. *Hum. Mol. Genet.* 27:3747–60
28. de la Cruz MV, Anselmi G, Cisneros F, Reinhold M, Portillo B, Espino-Vela J. 1959. An embryologic explanation for the corrected transposition of the great vessels: additional description of the main anatomic features of this malformation and its varieties. *Am. Heart J.* 57:104–17
29. de la Cruz MV, Castillo MM, Villavicencio L, Valencia A, Moreno-Rodriguez RA. 1997. Primitive interventricular septum, its primordium, and its contribution in the definitive interventricular septum: in vivo labelling study in the chick embryo heart. *Anat. Rec.* 247:512–20
30. de Lange FJ, Moorman AFM, Anderson RH, Männer J, Soufan AT, et al. 2004. Lineage and morphogenetic analysis of the cardiac valves. *Circ. Res.* 95:645–54
31. de Soysa TY, Ranade SS, Okawa S, Ravichandran S, Huang Y, et al. 2019. Single-cell analysis of cardiogenesis reveals basis for organ-level developmental defects. *Nature* 572:120–24
32. Desgrange A, Le Garrec J-F, Bernheim S, Bønnelykke TH, Meilhac SM. 2020. Transient nodal signaling in left precursors coordinates opposed asymmetries shaping the heart loop. *Dev. Cell* 55:413–31.e6
33. Desgrange A, Lokmer J, Marchiol C, Houyel L, Meilhac SM. 2019. Standardised imaging pipeline for phenotyping mouse laterality defects and associated heart malformations, at multiple scales and multiple stages. *Dis. Model. Mech.* 12:dmm038356

34. Domínguez JN, Meilhac SM, Bland YS, Buckingham ME, Brown NA. 2012. Asymmetric fate of the posterior part of the second heart field results in unexpected left/right contributions to both poles of the heart. *Circ. Res.* 111:1323–35
35. Eley L, Alqahtani AM, MacGrogan D, Richardson RV, Murphy L, et al. 2018. A novel source of arterial valve cells linked to bicuspid aortic valve without raphe in mice. *eLife* 7:e34110
36. Ellesøe SG, Workman CT, Bouvagnet P, Loffredo CA, McBride KL, et al. 2018. Familial co-occurrence of congenital heart defects follows distinct patterns. *Eur. Heart J.* 39:1015–22
37. Franco D, Meilhac SM, Christoffels VM, Kispert A, Buckingham M, Kelly RG. 2006. Left and right ventricular contributions to the formation of the interventricular septum in the mouse heart. *Dev. Biol.* 294:366–75
38. Franklin RCG, Béland MJ, Colan SD, Walters HL, Aiello VD, et al. 2017. Nomenclature for congenital and paediatric cardiac disease: the International Paediatric and Congenital Cardiac Code (IPCCC) and the eleventh iteration of the International Classification of Diseases (ICD-11). *Cardiol. Young* 27:1872–938
39. Furtado MB, Biben C, Shiratori H, Hamada H, Harvey RP. 2011. Characterization of *Pitx2c* expression in the mouse heart using a reporter transgene. *Dev. Dyn.* 240:195–203
40. Garg V, Muth AN, Ransom JF, Schluterman MK, Barnes R, et al. 2005. Mutations in *NOTCH1* cause aortic valve disease. *Nature* 437:270–74
41. Gaussin V, Van de Putte T, Mishina Y, Hanks MC, Zwijsen A, et al. 2002. Endocardial cushion and myocardial defects after cardiac myocyte-specific conditional deletion of the bone morphogenetic protein receptor ALK3. *PNAS* 99:2878–83
42. Goddeeris MM, Schwartz R, Klingensmith J, Meyers EN. 2007. Independent requirements for Hedgehog signaling by both the anterior heart field and neural crest cells for outflow tract development. *Development* 134:1593–604
43. Goldmuntz E, Bamford R, Karkera JD, dela Cruz J, Roessler E, Muenke M. 2002. *CFC1* mutations in patients with transposition of the great arteries and double-outlet right ventricle. *Am. J. Hum. Genet.* 70:776–80
44. Guimier A, Gabriel GC, Bajolle F, Tsang M, Liu H, et al. 2015. *MMP21* is mutated in human heterotaxy and is required for normal left-right asymmetry in vertebrates. *Nat. Genet.* 47:1260–63
45. Harh JY, Paul MH. 1975. Experimental cardiac morphogenesis. I. Development of the ventricular septum in the chick. *J. Embryol. Exp. Morphol.* 33:13–28
46. Harrelson Z, Kelly RG, Goldin SN, Gibson-Brown JJ, Bollag RJ, et al. 2004. *Tbx2* is essential for patterning the atrioventricular canal and for morphogenesis of the outflow tract during heart development. *Development* 131:5041–52
47. Hiermeier F, Männer J. 2017. Kinking and torsion can significantly improve the efficiency of valveless pumping in periodically compressed tubular conduits. Implications for understanding of the form-function relationship of embryonic heart tubes. *J. Cardiovasc. Dev. Dis.* 4:19
48. Hinton RB, Lincoln J, Deutsch GH, Osinska H, Manning PB, et al. 2006. Extracellular matrix remodeling and organization in developing and diseased aortic valves. *Circ. Res.* 98:1431–38
49. Hinton RB, Yutzey KE. 2011. Heart valve structure and function in development and disease. *Annu. Rev. Physiol.* 73:29–46
50. Hoffmann AD, Peterson MA, Friedland-Little JM, SA Anderson, Moskowitz IP. 2009. Sonic hedgehog is required in pulmonary endoderm for atrial septation. *Development* 136:1761–70
51. Hoffmann AD, Yang XH, Burnicka-Turek O, Bosman JD, Ren X, et al. 2014. *Foxf* genes integrate *Tbx5* and Hedgehog pathways in the second heart field for cardiac septation. *PLOS Genet.* 10:e1004604
52. Homasy J, Zaidi S, Shen Y, Ware JS, Samocha KE, et al. 2015. De novo mutations in congenital heart disease with neurodevelopmental and other congenital anomalies. *Science* 350:1262–66
53. Houyel L, Bajolle F, Capderou A, Laux D, Parisot P, Bonnet D. 2013. The pattern of the coronary arterial orifices in hearts with congenital malformations of the outflow tracts: a marker of rotation of the outflow tract during cardiac development? *J. Anat.* 222:349–57
54. Houyel L, Khoshnood B, Anderson RH, Lelong N, Thieulin A-C, et al. 2011. Population-based evaluation of a suggested anatomic and clinical classification of congenital heart defects based on the International Paediatric and Congenital Cardiac Code. *Orphanet J. Rare Dis.* 6:64

55. Ionescu-Ittu R, Mackie AS, Abrahamowicz M, Pilote L, Tchervenkov C, et al. 2010. Valvular operations in patients with congenital heart disease: increasing rates from 1988 to 2005. *Ann. Thorac. Surg.* 90:1563–69
56. Jacobs JP, Anderson RH, Weinberg PM, Walters HL, Tchervenkov CI, et al. 2007. The nomenclature, definition and classification of cardiac structures in the setting of heterotaxy. *Cardiol. Young* 17(Suppl. 2):1–28
57. Jiang X, Rowitch DH, Soriano P, McMahon AP, Sucov HM. 2000. Fate of the mammalian cardiac neural crest. *Development* 127:1607–16
58. Jin SC, Homsy J, Zaidi S, Lu Q, Morton S, et al. 2017. Contribution of rare inherited and de novo variants in 2,871 congenital heart disease probands. *Nat. Genet.* 49:1593–601
59. Kanani M, Moorman AFM, Cook AC, Webb S, Brown NA, et al. 2005. Development of the atrioventricular valves: clinicomorphological correlations. *Ann. Thorac. Surg.* 79:1797–804
60. Kelly RG, Brown NA, Buckingham ME. 2001. The arterial pole of the mouse heart forms from Fgf10-expressing cells in pharyngeal mesoderm. *Dev. Cell* 1:435–40
61. Khoshnood B, Lelong N, Houyel L, Thieulin A-C, Jouannic J-M, et al. 2012. Prevalence, timing of diagnosis and mortality of newborns with congenital heart defects: a population-based study. *Heart* 98:1667–73
62. Kim RY, Robertson EJ, Solloway MJ. 2001. Bmp6 and Bmp7 are required for cushion formation and septation in the developing mouse heart. *Dev. Biol.* 235:449–66
63. Kirby ML, Gale TF, Stewart DE. 1983. Neural crest cells contribute to normal aorticopulmonary septation. *Science* 220:1059–61
64. Koshiba-Takeuchi K, Mori AD, Kaynak BL, Cebra-Thomas J, Sukonnik T, et al. 2009. Reptilian heart development and the molecular basis of cardiac chamber evolution. *Nature* 461:95–98
65. Kramer TC. 1942. The partitioning of the truncus and conus and the formation of the membranous portion of the interventricular septum in the human heart. *Am. J. Anat.* 71:343–70
66. Krishnan A, Samtani R, Dhanantwari P, Lee E, Yamada S, et al. 2014. A detailed comparison of mouse and human cardiac development. *Pediatr. Res.* 76:500–7
67. LaHaye S, Lincoln J, Garg V. 2014. Genetics of valvular heart disease. *Curr. Cardiol. Rep.* 16:487
68. Lamers WH, Virágh S, Wessels A, Moorman AF, Anderson RH. 1995. Formation of the tricuspid valve in the human heart. *Circulation* 91:111–21
69. Lamers WH, Wessels A, Verbeek FJ, Moorman AF, Virágh S, et al. 1992. New findings concerning ventricular septation in the human heart: implications for maldevelopment. *Circulation* 86:1194–205
70. Le Garrec J-F, Domínguez JN, Desgrange A, Ivanovitch KD, Raphaël E, et al. 2017. A predictive model of asymmetric morphogenesis from 3D reconstructions of mouse heart looping dynamics. *eLife* 6:e28951
71. Lescroart F, Kelly RG, Le Garrec J-F, Nicolas J-F, Meilhac SM, Buckingham M. 2010. Clonal analysis reveals common lineage relationships between head muscles and second heart field derivatives in the mouse embryo. *Development* 137:3269–79
72. Lescroart F, Mohun T, Meilhac SM, Bennett M, Buckingham M. 2012. Lineage tree for the venous pole of the heart: clonal analysis clarifies controversial genealogy based on genetic tracing. *Circ. Res.* 111:1313–22
73. Lescroart F, Wang X, Lin X, Swedlund B, Gargouri S, et al. 2018. Defining the earliest step of cardiovascular lineage segregation by single-cell RNA-seq. *Science* 359:1177–81
74. Lev M, Bharati S, Meng CC, Libberthson RR, Paul MH, Idriss F. 1972. A concept of double-outlet right ventricle. *J. Thorac. Cardiovasc. Surg.* 64:271–81
75. Li G, Xu A, Sim S, Priest JR, Tian X, et al. 2016. Transcriptomic profiling maps anatomically patterned subpopulations among single embryonic cardiac cells. *Dev. Cell* 39:491–507
76. Li QY, Newbury-Ecob RA, Terrett JA, Wilson DI, Curtis AR, et al. 1997. Holt-Oram syndrome is caused by mutations in TBX5, a member of the *Brachyury* (*T*) gene family. *Nat. Genet.* 15:21–29
77. Lin AE, Krikov S, Riehle-Colarusso T, Frías JL, Belmont J, et al. 2014. Laterality defects in the national birth defects prevention study (1998–2007): birth prevalence and descriptive epidemiology. *Am. J. Med. Genet. A* 164A:2581–91
78. Lincoln J, Alfieri CM, Yutzey KE. 2004. Development of heart valve leaflets and supporting apparatus in chicken and mouse embryos. *Dev. Dyn.* 230:239–50

79. Liu W, Selever J, Wang D, Lu M-F, Moses KA, et al. 2004. Bmp4 signaling is required for outflow-tract septation and branchial-arch artery remodeling. *PNAS* 101:4489–94
80. Liu X, Tobita K, Francis RJB, Lo CW. 2013. Imaging techniques for visualizing and phenotyping congenital heart defects in murine models. *Birth Defects Res. C* 99:93–105
81. Liu X, Yagi H, Saeed S, Bais AS, Gabriel GC, et al. 2017. The complex genetics of hypoplastic left heart syndrome. *Nat. Genet.* 49:1152–59
82. Liu Y, Chen S, Zühlke L, Black GC, Choy M-K, et al. 2019. Global birth prevalence of congenital heart defects 1970–2017: updated systematic review and meta-analysis of 260 studies. *Int. J. Epidemiol.* 48:455–63
83. Lopez L, Houyel L, Colan SD, Anderson RH, Béland MJ, et al. 2018. Classification of ventricular septal defects for the eleventh iteration of the International Classification of Diseases—striving for consensus: a report from the International Society for Nomenclature of Paediatric and Congenital Heart Disease. *Ann. Thorac. Surg.* 106:1578–89
84. Luna-Zurita L, Prados B, Grego-Bessa J, Luxán G, del Monte G, et al. 2010. Integration of a Notch-dependent mesenchymal gene program and Bmp2-driven cell invasiveness regulates murine cardiac valve formation. *J. Clin. Investig.* 120:3493–507
85. Ma L, Lu M-F, Schwartz RJ, Martin JF. 2005. Bmp2 is essential for cardiac cushion epithelial-mesenchymal transition and myocardial patterning. *Development* 132:5601–11
86. MacGrogan D, Münch J, de la Pompa JL. 2018. Notch and interacting signalling pathways in cardiac development, disease, and regeneration. *Nat. Rev. Cardiol.* 15:685–704
87. Männer J, Seidl W, Steding G. 1993. Correlation between the embryonic head flexures and cardiac development: an experimental study in chick embryos. *Anat. Embryol.* 188:269–85
88. Marelli AJ, Ionescu-Ittu R, Mackie AS, Guo L, Dendukuri N, Kaouache M. 2014. Lifetime prevalence of congenital heart disease in the general population from 2000 to 2010. *Circulation* 130:749–56
89. Marino BS, Lipkin PH, Newburger JW, Peacock G, Gerdes M, et al. 2012. Neurodevelopmental outcomes in children with congenital heart disease: evaluation and management; a scientific statement from the American Heart Association. *Circulation* 126:1143–72
90. Markwald RR, Fitzharris TP, Manasek FJ. 1977. Structural development of endocardial cushions. *Am. J. Anat.* 148:85–119
91. Meilhac SM, Esner M, Kelly RG, Nicolas J-F, Buckingham ME. 2004. The clonal origin of myocardial cells in different regions of the embryonic mouse heart. *Dev. Cell* 6:685–98
92. Meilhac SM, Esner M, Kerszberg M, Moss JE, Buckingham ME. 2004. Oriented clonal cell growth in the developing mouse myocardium underlies cardiac morphogenesis. *J. Cell Biol.* 164:97–109
93. Merscher S, Funke B, Epstein JA, Heyer J, Puech A, et al. 2001. *TBX1* is responsible for cardiovascular defects in velo-cardio-facial/DiGeorge syndrome. *Cell* 104:619–29
94. Midgett M, Thornburg K, Rugonyi S. 2017. Blood flow patterns underlie developmental heart defects. *Am. J. Physiol. Heart Circ. Physiol.* 312:H632–42
95. Mifflin JJ, Dupuis LE, Alcalá NE, Russell LG, Kern CB. 2018. Intercalated cushion cells within the cardiac outflow tract are derived from the myocardial troponin T type 2 (*Tnnt2*) Cre lineage. *Dev. Dyn.* 247:1005–17
96. Mohapatra B, Casey B, Li H, Ho-Dawson T, Smith L, et al. 2009. Identification and functional characterization of NODAL rare variants in heterotaxy and isolated cardiovascular malformations. *Hum. Mol. Genet.* 18:861–71
97. Mohun TJ, Anderson RH. 2020. 3D anatomy of the developing heart: understanding ventricular septation. *Cold Spring Harb. Perspect. Biol.* 12:a037465
98. Mohun TJ, Brown NA, Anderson RH. 2016. Development of the heart and great vessels. In *Kaufman's Atlas of Mouse Development Supplement: With Coronal Sections*, ed R Baldock, J Bard, DR Davidson, G Morriss-Kay, pp. 95–109. Boston: Academic
99. Moore-Morris T, van Vliet PP, Andelfinger G, Pucaet M. 2018. Role of epigenetics in cardiac development and congenital diseases. *Physiol. Rev.* 98:2453–75
100. Moreau JLM, Kesteven S, Martin EMMA, Lau KS, Yam MX, et al. 2019. Gene-environment interaction impacts on heart development and embryo survival. *Development* 146:dev172957

101. Morton PD, Ishibashi N, Jonas RA. 2017. Neurodevelopmental abnormalities and congenital heart disease: insights into altered brain maturation. *Circ. Res.* 120:960–77
102. Mostefa-Kara M, Bonnet D, Belli E, Fadel E, Houyel L. 2015. Anatomy of the ventricular septal defect in outflow tract defects: similarities and differences. *J. Thorac. Cardiovasc. Surg.* 149:682–88.e1
103. Neptune ER, Frischmeyer PA, Arking DE, Myers L, Bunton TE, et al. 2003. Dysregulation of TGF- β activation contributes to pathogenesis in Marfan syndrome. *Nat. Genet.* 33:407–11
104. Niederreither K, Subbarayan V, Dollé P, Chambon P. 1999. Embryonic retinoic acid synthesis is essential for early mouse post-implantation development. *Nat. Genet.* 21:444–48
105. Norris DP, Brennan J, Bikoff EK, Robertson EJ. 2002. The Foxh1-dependent autoregulatory enhancer controls the level of Nodal signals in the mouse embryo. *Development* 129:3455–68
106. Odelin G, Faure E, Couplier F, Di Bonito M, Bajolle F, et al. 2018. Krox20 defines a subpopulation of cardiac neural crest cells contributing to arterial valves and bicuspid aortic valve. *Development* 145:dev151944
107. Oosthoek PW, Wenink AC, Vrolijk BC, Wisse LJ, DeRuiter MC, et al. 1998. Development of the atrioventricular valve tension apparatus in the human heart. *Anat. Embryol.* 198:317–29
108. Øyen N, Poulsen G, Boyd HA, Wohlfahrt J, Jensen PKA, Melbye M. 2009. Recurrence of congenital heart defects in families. *Circulation* 120:295–301
109. Patten BM. 1922. The formation of the cardiac loop in the chick. *Am. J. Anat.* 30:373–97
110. Peyvandi S, Latal B, Miller SP, McQuillen PS. 2019. The neonatal brain in critical congenital heart disease: insights and future directions. *Neuroimage* 185:776–82
111. Phillips HM, Mahendran P, Singh E, Anderson RH, Chaudhry B, Henderson DJ. 2013. Neural crest cells are required for correct positioning of the developing outflow cushions and pattern the arterial valve leaflets. *Cardiovasc. Res.* 99:452–60
112. Pierpont ME, Brueckner M, Chung WK, Garg V, Lacro RV, et al. 2018. Genetic basis for congenital heart disease: revisited: a scientific statement from the American Heart Association. *Circulation* 138:e653–711
113. Ryckebusch L, Wang Z, Bertrand N, Lin S-C, Chi X, et al. 2008. Retinoic acid deficiency alters second heart field formation. *PNAS* 105:2913–18
114. Saijoh Y, Oki S, Ohishi S, Hamada H. 2003. Left-right patterning of the mouse lateral plate requires nodal produced in the node. *Dev. Biol.* 256:160–72
115. Sanford LP, Ormsby I, Gittenberger-de Groot AC, Sariola H, Friedman R, et al. 1997. TGF β 2 knockout mice have multiple developmental defects that are non-overlapping with other TGF β knockout phenotypes. *Development* 124:2659–70
116. Shieh JTC, Bittles AH, Hudgins L. 2012. Consanguinity and the risk of congenital heart disease. *Am. J. Med. Genet. A* 158A:1236–41
117. Shirai M, Imanaka-Yoshida K, Schneider MD, Schwartz RJ, Morisaki T. 2009. T-box 2, a mediator of Bmp-Smad signaling, induced hyaluronan synthase 2 and Tgf β 2 expression and endocardial cushion formation. *PNAS* 106:18604–9
118. Shiratori H, Hamada H. 2006. The left-right axis in the mouse: from origin to morphology. *Development* 133:2095–104
119. Sifrim A, Hitz M-P, Wilsdon A, Breckpot J, Turki SHA, et al. 2016. Distinct genetic architectures for syndromic and nonsyndromic congenital heart defects identified by exome sequencing. *Nat. Genet.* 48:1060–65
120. Sigmon ER, Kelleman M, Susi A, Nylund CM, Oster ME. 2019. Congenital heart disease and autism: a case-control study. *Pediatrics* 144:e20184114
121. Sizarov A, Baldwin H, Srivastava D, Moorman AF. 2016. Development of the heart: morphogenesis, growth, and molecular regulation of differentiation. In *Moss and Adams' Heart Disease in Infants, Children, and Adolescents, Including the Fetus and Young Adult*, ed. HD Allen, RE Shaddy, DJ Penny, TF Feltes, F Cetta, pp. 1–54. Philadelphia: Wolters Kluwer
122. Sizarov A, Lamers WH, Mohun TJ, Brown NA, Anderson RH, Moorman AFM. 2012. Three-dimensional and molecular analysis of the arterial pole of the developing human heart. *J. Anat.* 220:336–49

123. Sizarov A, Ya J, de Boer BA, Lamers WH, Christoffels VM, Moorman AFM. 2011. Formation of the building plan of the human heart: morphogenesis, growth, and differentiation. *Circulation* 123:1125–35
124. Snarr BS, Wirrig EE, Phelps AL, Trusk TC, Wessels A. 2007. A spatiotemporal evaluation of the contribution of the dorsal mesenchymal protrusion to cardiac development. *Dev. Dyn.* 236:1287–94
125. Stottmann RW, Choi M, Mishina Y, Meyers EN, Klingensmith J. 2004. BMP receptor IA is required in mammalian neural crest cells for development of the cardiac outflow tract and ventricular myocardium. *Development* 131:2205–18
126. Sugi Y, Ito N, Szebenyi G, Myers K, Fallon JF, et al. 2003. Fibroblast growth factor (FGF)-4 can induce proliferation of cardiac cushion mesenchymal cells during early valve leaflet formation. *Dev. Biol.* 258:252–63
127. Sullivan PM, Dervan LA, Reiger S, Buddhe S, Schwartz SM. 2015. Risk of congenital heart defects in the offspring of smoking mothers: a population-based study. *J. Pediatr.* 166:978–84.e2
128. Supp DM, Witte DP, Potter SS, Brueckner M. 1997. Mutation of an axonemal dynein affects left-right asymmetry in inversus viscerum mice. *Nature* 389:963–66
129. Tang S, Snider P, Firulli AB, Conway SJ. 2010. Trigenic neural crest-restricted Smad7 over-expression results in congenital craniofacial and cardiovascular defects. *Dev. Biol.* 344:233–47
130. Thiene G, Frescura C. 2010. Anatomical and pathophysiological classification of congenital heart disease. *Cardiovasc. Pathol.* 19:259–74
131. Thompson RP, Abercrombie V, Wong M. 1987. Morphogenesis of the truncus arteriosus of the chick embryo heart: movements of autoradiographic tattoos during septation. *Anat. Rec.* 218:434–40
132. Togi K, Yoshida Y, Matsumae H, Nakashima Y, Kita T, Tanaka M. 2006. Essential role of *Hand2* in interventricular septum formation and trabeculation during cardiac development. *Biochem. Biophys. Res. Commun.* 343:144–51
133. Tremblay C, Loomba RS, Frommelt PC, Perrin D, Spicer DE, et al. 2017. Segregating bodily isomerism or heterotaxy: potential echocardiographic correlations of morphological findings. *Cardiol. Young* 27:1470–80
134. Tsao P-C, Lee Y-S, Jeng M-J, Hsu J-W, Huang K-L, et al. 2017. Additive effect of congenital heart disease and early developmental disorders on attention-deficit/hyperactivity disorder and autism spectrum disorder: a nationwide population-based longitudinal study. *Eur. Child Adolesc. Psychiatry* 26:1351–59
135. Tyser RCV, Ibarra-Soria X, McDole K, Arcot Jayaram S, Godwin J, et al. 2021. Characterization of a common progenitor pool of the epicardium and myocardium. *Science* 371:eabb2986
136. Van Mierop LH, Gessner IH. 1972. Pathogenetic mechanisms in congenital cardiovascular malformations. *Prog. Cardiovasc. Dis.* 15:67–85
137. Van Praagh R. 1972. The segmental approach to diagnosis in congenital heart disease. *Birth Defects Orig. Art. Ser.* 8:4–23
138. Van Praagh S, Davidoff A, Chin A, Shiel F, Reynolds J, Vanpraagh R. 1982. Double outlet right ventricle: anatomic types and developmental implications based on a study of 101 autopsied cases. *Coeur* 13:390–439
139. Van Praagh R, Ongley PA, Swan HJ. 1964. Anatomic types of single or common ventricle in man: morphologic and geometric aspects of 60 necropsied cases. *Am. J. Cardiol.* 13:367–86
140. Waldo KL, Hutson MR, Stadt HA, Zdanowicz M, Zdanowicz J, Kirby ML. 2005. Cardiac neural crest is necessary for normal addition of the myocardium to the arterial pole from the secondary heart field. *Dev. Biol.* 281:66–77
141. Waldo KL, Kumiski DH, Wallis KT, Stadt HA, Hutson MR, et al. 2001. Conotruncal myocardium arises from a secondary heart field. *Development* 128:3179–88
142. Waxman JS, Keegan BR, Roberts RW, Poss KD, Yelon D. 2008. Hoxb5b acts downstream of retinoic acid signaling in the forelimb field to restrict heart field potential in zebrafish. *Dev. Cell* 15:923–34
143. Webb S, Brown NA, Anderson RH. 1998. Formation of the atrioventricular septal structures in the normal mouse. *Circ. Res.* 82:645–56
144. Wessels A, van den Hoff MJB, Adamo RF, Phelps AL, Lockhart MM, et al. 2012. Epicardially derived fibroblasts preferentially contribute to the parietal leaflets of the atrioventricular valves in the murine heart. *Dev. Biol.* 366:111–24

145. Ya J, van den Hoff MJ, de Boer PA, Tesink-Taekema S, Franco D, et al. 1998. Normal development of the outflow tract in the rat. *Circ. Res.* 82:464–72
146. Yelbuz TM, Waldo KL, Kumiski DH, Stadt HA, Wolfe RR, et al. 2002. Shortened outflow tract leads to altered cardiac looping after neural crest ablation. *Circulation* 106:504–10
147. Yotti R, Seidman CE, Seidman JG. 2019. Advances in the genetic basis and pathogenesis of sarcomere cardiomyopathies. *Annu. Rev. Genom. Hum. Genet.* 20:129–53
148. Yu CKH, Teoh TG, Robinson S. 2006. Obesity in pregnancy. *BjOG* 113:1117–25
149. Zaffran S, Kelly RG, Meilhac SM, Buckingham ME, Brown NA. 2004. Right ventricular myocardium derives from the anterior heart field. *Circ. Res.* 95:261–68
150. Zaidi S, Brueckner M. 2017. Genetics and genomics of congenital heart disease. *Circ. Res.* 120:923–40
151. Zhang Z, Huynh T, Baldini A. 2006. Mesodermal expression of *Tbx1* is necessary and sufficient for pharyngeal arch and cardiac outflow tract development. *Development* 133:3587–95
152. Zhou L, Liu J, Olson P, Zhang K, Wynne J, Xie L. 2015. *Tbx5* and *Osr1* interact to regulate posterior second heart field cell cycle progression for cardiac septation. *J. Mol. Cell. Cardiol.* 85:1–12

RELATED RESOURCES

- Amst. Med. Cent. 2021. *3D Atlas of Human Embryology*. <https://www.3dembryoatlas.com>
- Cent. Dis. Control Prev. 2021. Specific congenital heart defects. *Centers for Disease Control and Prevention*. <https://www.cdc.gov/ncbddd/heartdefects/specificdefects.html>
- eMouseAtlas Proj. 2021. *eMouseAtlas*. <http://www.emouseatlas.org>
- Endow. Hum. Dev. 2021. The Virtual Human Embryo Project. *Endowment for Human Development*. <https://www.ehd.org/virtual-human-embryo/about.php>
- Hill MA. 2021. Embryonic development. *University of New South Wales*. https://embryology.med.unsw.edu.au/embryology/index.php/Embryonic_Development
- Int. Soc. Nomencl. Paediatr. Congenit. Heart Dis. 2021. Home page. *International Society for Nomenclature of Paediatric and Congenital Heart Disease*. <https://www.ipccc.net>
- Smith B. 2016. *The Multi-Dimensional Human Embryo*. <http://embryo.soad.umich.edu>